UNIVERSIDADE FEDERAL DE OURO PRETO
ESCOLA DE MINAS
DEPARTAMENTO DE GEOLOGIA

PROGRAMA DE PÓS-GRADUAÇÃO EM EVOLUÇÃO CRUSTAL
E RECURSOS NATURAIS

Geologia Ambiental e Conservação de Recursos Naturais

DISSERTAÇÃO DE MESTRADO

ONGOING LANDSCAPE TRANSIENCE IN THE EASTERN AMAZON CRATON CONSISTENT WITH LITHOLOGIC CONTROL OF BASE LEVEL

Camila Morato Fadul

Ouro Preto, dezembro de 2021

ONGOING LANDSCAPE TRANSIENCE IN THE EASTERN AMAZON CRATON CONSISTENT WITH LITHOLOGIC CONTROL OF BASE LEVEL

FUNDAÇÃO UNIVERSIDADE FEDERAL DE OURO PRETO

Reitora

Cláudia Aparecida Marliére de Lima

Vice-Reitor

Hermínio Arias Nalini Júnior

Pró-Reitor de Pesquisa e Pós-Graduação

Sérgio Francisco de Aquino

ESCOLA DE MINAS

Diretor

José Alberto Naves Cocota Junior

Vice-Diretor

Cláudio Eduardo Lana

DEPARTAMENTO DE GEOLOGIA

Chefe

Edison Tazava

EVOLUÇÃO CRUSTAL E RECURSOS NATURAIS

CONTRIBUIÇÕES ÀS CIÊNCIAS DA TERRA – VOL. 80

DISSERTAÇÃO MESTRADO

Nº 431

ONGOING LANDSCAPE TRANSIENCE IN THE EASTERN AMAZON CRATON CONSISTENT WITH LITHOLOGIC CONTROL OF BASE LEVEL

Camila Morato Fadul

Orientador

Prof. Dr. Pedro Fonseca de Almeida e Val

Dissertação apresentada ao Programa de Pós-Graduação em Evolução Crustal e Recursos Naturais do Departamento de Geologia da Escola de Minas da Universidade Federal de Ouro Preto como requisito parcial à obtenção do Título de Mestre em Geologia.

Área de concentração: Geologia Ambiental e Conservação de Recursos Naturais

OURO PRETO

2021

Universidade Federal de Ouro Preto – http://www.ufop.br
Escola de Minas - http://www.em.ufop.br
Departamento de Geologia - http://www.degeo.ufop.br/
Programa de Pós-Graduação em Evolução Crustal e Recursos Naturais
Campus Morro do Cruzeiro s/n - Bauxita
35.400-000 Ouro Preto, Minas Gerais
Tel. (31) 3559-1600, Fax: (31) 3559-1606 e-mail: pgrad@degeo.ufop.br

ISSN

Depósito Legal na Biblioteca Nacional

1ª Edição

SISBIN - SISTEMA DE BIBLIOTECAS E INFORMAÇÃO

F146o Fadul, Camila Morato.
Ongoing landscape transience in the eastern Amazon Craton consistent with lithologic control of base level. [manuscrito] / Camila Morato Fadul. - 2021.
63 f. (Série: M)

Orientador: Prof. Dr. Pedro Val.
Dissertação (Mestrado Acadêmico). Universidade Federal de Ouro Preto. Departamento de Geologia. Programa de Pós-Graduação em Evolução Crustal e Recursos Naturais.
Área de Concentração: Geologia Ambiental e Conservação de Recursos Naturais – Garn.

1. Geomorfologia - Nível de base. 2. Paisagens - Evolução. 3. Crátons. 4. Petrologia. I. Val, Pedro. II. Universidade Federal de Ouro Preto. III. Título.

CDU 551.435.12

Bibliotecário(a) Responsável: Sione Galvão Rodrigues - CRB6 / 2526

http://www.sisbin.ufop.br

MINISTÉRIO DA EDUCAÇÃO
UNIVERSIDADE FEDERAL DE OURO PRETO
REITORIA
ESCOLA DE MINAS
COORDENACAO DO PROGRAMA DE POS-GRADUACAO
EM EVOLUCAO CRUSTAL

FOLHA DE APROVAÇÃO

Camila Morato Fadul

Ongoing landscape transience in the eastern Amazon Craton consistent with lithologic control of base level

Dissertação apresentada ao Programa de Pós-Graduação em Evolução Crustal e Recursos Naturais da Universidade Federal
de Ouro Preto como requisito parcial para obtenção do título de Mestre em Ciências Naturais.

Aprovada em 17 de dezembro de 2021.

Membros da banca

Prof. Dr. Pedro Fonseca de Almeida e Val- Orientador(a) Universidade Federal de Ouro Preto
Prof. Dr. Fernando do Nascimento Pupim - Universidade Federal de São Paulo
Dr. Daniel Peifer Bezerra - Universidade Federal de Minas Gerais

Prof. Dr. Pedro Fonseca de Almeida, orientador do trabalho, aprovou a versão final e autorizou seu depósito no Repositório Institucional da UFOP em 24/05/2022.

Documento assinado eletronicamente por **Isaac Daniel Rudnitzki**, **COORDENADOR(A) DE CURSO DE PÓS-GRADUAÇÃO EM EVOLUÇÃO CRUSTAL E RECURSOS NATURAIS**, em 23/08/2022, às 12:37, conforme horário oficial de Brasília, com fundamento no art. 6º, § 1º, do Decreto nº 8.539, de 8 de outubro de 2015.

A autenticidade deste documento pode ser conferida no site http://sei.ufop.br/sei/controlador_externo.php?acao=documento_conferir&id_orgao_acesso_externo=0 , informando o código verificador **0380287** e o código CRC **F4B1EFAF**.

R. Diogo de Vasconcelos, 122, - Bairro Pilar Ouro Preto/MG, CEP 35400-000
Telefone: (31)3559-1605 - www.ufop.br

Agradecimentos

Fico feliz em agradecer ao meu orientador Pedro Val pela oportunidade de fazer parte deste projeto e por todas as sugestões, comentários e desafios científicos importantes que me inspiraram ao longo do mestrado. Além disso, a experiência de trabalho de campo na floresta amazônica e profundo conhecimento da paisagem e métodos computacionais para sua análise.

Sou especialmente grata à minha família e amigos por estarem ao meu lado com amor e todo tipo de apoio.

À Prof. Gláucia Queiroga e Daiana Mendes de Oliveira Rossi, da pós-graduação, por toda a disponibilidade e atenção durante o mestrado.

A Daniel Piefer pelas excelentes aulas de Geomorfologia Quantitativa.

Ao Fabiano Pupim pela primeira oportunidade de estudar na USP.

À Universidade Federal de Ouro Preto e ao Departamento de Geologia pela oportunidade de continuar minha profissionalização como pesquisadora.

À Coordenação de Aperfeiçoamento de Pessoal de Nível Superior (Capes) pela concessão da bolsa de mestrado.

Sumário

Lista de Figuras

Resumo

No leste do Escudo das Guianas, região pertencente ao cráton Amazonas, são observadas características geomórficas, como capturas de drenagem, *knickpoints*, paleocanais, migração dos divisores de drenagem e *wind-gaps* normalmente interpretados como sendo o resultado de mudanças climáticas e processos tectônicos intraplaca. Além desses processos, é de se esperar que em regiões cratônicas, a presença de diferentes litologias atue como um gatilho para gerar paisagens transientes. Os rios que drenam o escudo fluem em direção às rochas sedimentares da bacia Amazônica através de uma Escarpa Principal (EP) marcando uma transição litológica formada por arenitos de alta resistência erosiva pertencentes às unidades basais da Bacia Sedimentar Amazônica. Por meio da análise geomorfológica quantitativa do relevo, *chi-plots, knickpoints* e declividade do rio, investigamos a influência de uma litologia resistente (arenitos do Grupo Trombetas) nos padrões de drenagem do escudo. Os resultados revelaram que rios de bacias com maior área de drenagem associado à menores distâncias percorridas sobre rochas resistentes da EP capturam bacias vizinhas. Para a evolução da paisagem do leste do Escudo das Guianas, argumentamos que, à medida que a queda do nível de base do rio Amazonas se propaga rio acima em direção à região de cabeceira do escudo, eles são retardados diferencialmente pelas rochas resistentes, gerando uma série de feições transientes como captura de drenagem, migração do divisor e disparidade entre as distâncias percorridas por *knickpoints*. A presença de feições geomórficas sistemáticas sugerem que este pode ser um importante mecanismo autogênico de controle do rearranjo da rede de drenagem na região Amazônica, bem como em outras paisagens cratônicas. A exumação prolongada de rochas resistentes em crátons pode manter as paisagens em desequilíbrio constante e oferecer um laboratório natural excepcional para estudar a dinâmica da paisagem associada ao tipo de rocha.

PALAVRAS-CHAVE: evolução de paisagem, geomorfologia, Escudo das Guianas, *knickpoints*, *wind-gaps*

Abstract

Geomorphic features such as drainage captures, knickpoints, paleochannels, and wind-gaps have long been observed in the Amazon region and typically thought to result from climate change and intraplate tectonics. The influence of rock type as a trigger of these landscape transients is largely overlooked. In the eastern Guiana Shield of the Amazon Craton, shield rivers cross over to the sedimentary rocks of the Amazon basin across a sharp lithologic transition before their confluence with the Amazon River. The transition in rock type is marked by an expressive Main Escarpment (ME) formed over highly resistant sandstones of the basal units of the Amazon Sedimentary Basin. Here, systematic patterns of divide migration and river captures are observed and provide a natural laboratory to study the influence of rock type in landscape transience in a cratonic setting. Through quantitative geomorphology analysis of relief, chi-plots, knickpoints, and river steepness, we investigate if this sharp lithologic transition contributed to the observed patterns of drainage rearrangement. The results revealed that rivers of larger drainage areas flowing across shorter lengths over the resistant rocks of the ME systematically capture neighboring basins. We argue that, as base level fall of the Amazon River migrates upstream into its tributaries draining the shield, they are differentially slowed down by the resistant rocks, generating a series of transients such as drainage capture, divide migration and disparity between the distances traveled by knickpoints. The widespread and systematic features suggest this could be an important autogenic mechanism controlling drainage network rearrangement in the Amazon region as well as other post-orogenic landscapes. The protracted exhumation of resistant rocks in cratons and continent interiors may keep landscapes in perpetual disequilibrium depending on their lithological complexity and offer an exceptional natural laboratory to study landscape dynamics associated with rock type.

KEY WORDS: landscape evolution, geomorphology, Guiana Shield, wind-gaps, knickpoints

CÁPITULO 1
INTRODUÇÃO

1.1 APRESENTAÇÃO

A região Amazônica possui a maior bacia de drenagem do mundo – bacia do Rio Amazonas. O rio Amazonas corta o continente Sul-Americano desde as regiões Andinas no extremo oeste do continente até desaguar no Oceano Atlântico. Na margem direita do médio curso do Rio Amazonas encontramos uma região elevada com baixa declividade, constituindo um platô na porção oriental do Escudo das Guianas. Esse platô apresenta feições geomórficas como *wind-gaps* (paleo-canais abandonados) e *knickpoints* (degraus topográficos ao longo do canal do rio) que indicam um desequilíbrio da paisagem, isso é, indica uma paisagem em estado transiente. A paisagem Amazônica está inserida numa região intracratônica em que o último evento tectônico ocorreu há pelo menos 500 Ma com a fragmentação do continente Gondwana (e.g. Scotese 2009). Nesse contexto, a dissertação em questão utiliza o levantamento bibliográfico da história de evolução do rio Amazonas e o estudo de feições geomórficas na porção oriental do Escudo das Guianas para analisar uma região que apresenta evidências de paisagem em desequilíbrio, com intuito de entender a evolução dos padrões da rede de drenagem na região amazônica e em paisagens cratônicas.

1.2 NATUREZA DO PROBLEMA

Apesar da área de estudo estar localizada numa região onde não ocorre processos tectônicos há centenas de milhões de anos, feições geomórficas são frequentes na Amazônia oriental, constituindo evidências de uma perturbação no nível de base regional e apontando para o desequilíbrio da paisagem atual.

A presença de *wind-gaps* e *knickpoints* em bacias hidrográficas comumente refletem mudanças no nível de base desencadeada por processos de soerguimento ou queda do nível de base como resultado de processos tectônicos ou climáticos (Whipple e Tucker, 1999; Crosby e Whipple, 2006; Gallen *et al*., 2011). A resposta da paisagem à mudança de nível de base ou captura de rio é acompanhada pela propagação de um pulso erosivo em direção à cabeceira, consumindo a paisagem e deixando feições radiais como registro (Fig. 1.1). A análises dos padrões das feições geomórficas na área de estudo mostrou que processos de queda de nível de base não explicam sozinhos a evolução da paisagem do escudo, o que nos leva a investigar outros fatores possíveis geradores de transiência.

No caso da região Amazônica, o caráter heterogêneo da litologia típica de grandes bacias de drenagem localizadas no interior continental pode gerar taxas de migração de *knickpoints* e tempos de

resposta entre bacias vizinhas diferentes (e.g., Harbor *et al*., 2005; Berlin and Anderson 2007). Em tais cenários, a complexidade litológica, principalmente a exumação de rochas resistentes, pode desencadear a migração de divisores de drenagem, reorganização dos rios em bacias vizinhas e a mudança na geometria e forma das bacias (Bernard *et al*., 2021). Além disso, os rios que drenam o escudo fluem em direção às rochas sedimentares da bacia Amazônica e cruzam uma Escarpa Principal (EP) que marca uma transição litológica formada por arenitos de alta resistência erosiva pertencentes às unidades basais da Bacia Sedimentar Amazônica. A partir desse dado, propomos nesse trabalho, por meio da análise geomorfológica quantitativa, investigar a influência de uma litologia resistente nos padrões de drenagem do Escudo das Guianas.

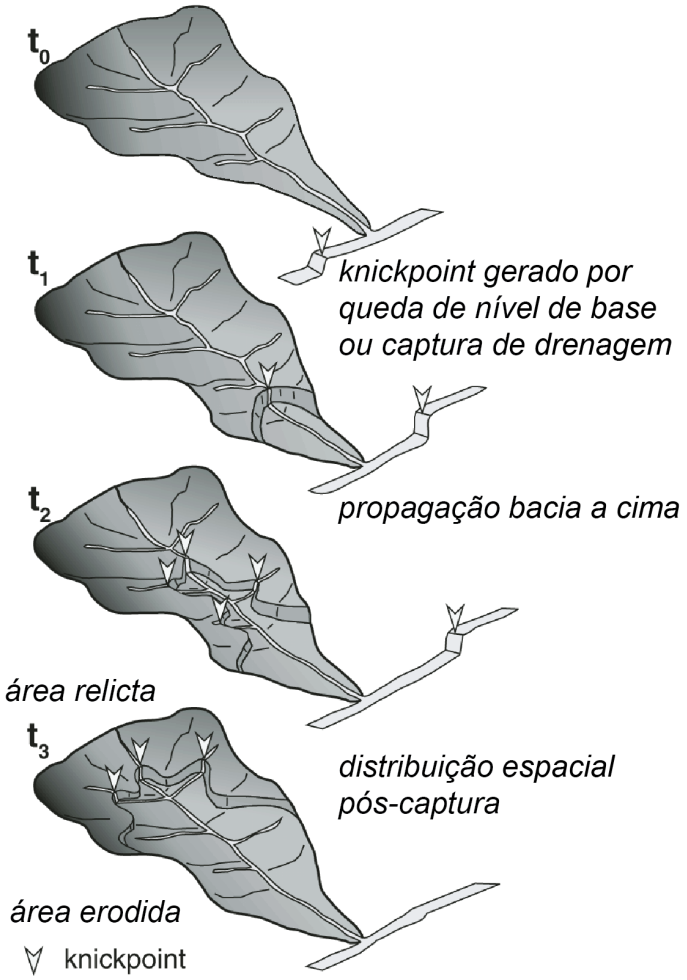

Figura 1.1- Modelo conceitual da resposta geomorfológica gerada por mudança no nível de base. Após evento de queda do nível de base ou captura de drenagem, *knickpoints* (setas brancas) se propagam como pulsos erosivos em direção à cabeceira consumindo a paisagem e formando feições radiais. **(**Imagem modificada de Gallen *et al*., 2013).

1.3 LOCALIZAÇÃO

A área de estudo escolhida para investigar feições transientes da paisagem está localizada na porção oriental do Escudo das Guianas. As bacias hidrográficas analisadas nesse trabalho estão situadas na porção noroeste do estado do Pará e oeste do Amapá, limitada pelos meridianos de longitude oeste 57°W -51°W, e latitude 3°N – 2°S, possui aproximadamente 400.000 km^2 (Figura 1.2).

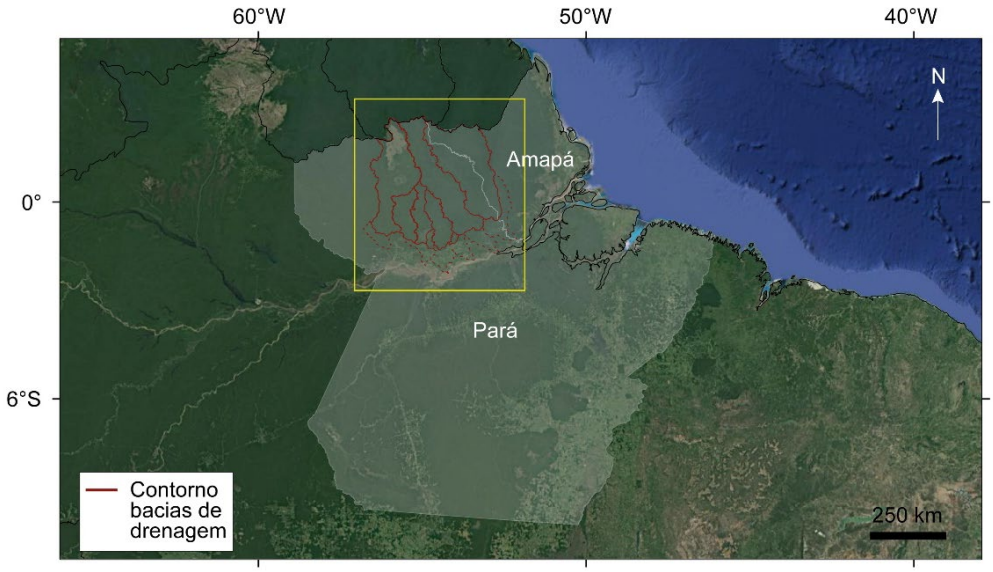

Figure 1.2- Imagem de satélite e localização da área de estudo (limitada pelo quadrado amarelo). (Google maps: https://www.google.com.br/maps. Acesso em 01/12/2021).

1.4 OBJETIVOS

O objetivo principal desse trabalho é determinar quais são os mecanismos responsáveis por gerar feições transientes da paisagem na porção oriental do Escudo das Guianas.

Para atingir o objetivo principal, será necessário atingir os seguintes objetivos específicos:

• Revisão bibliográfica da história de evolução do rio Amazonas;

• Mapeamento de feições transientes da paisagem;

• Obtenção de métricas geomórficas;

• Estudo do efeito litológico na área de estudo.

1.5 METODOLOGIA

1.5.1 Revisão bibliográfica

A revisão bibliográfica baseou-se em material disponível sobre os diversos assuntos relacionados à dissertação de mestrado, como a história de evolução do rio Amazonas, geologia regional do Cráton Amazonas e da Bacia Sedimentar do Amazonas, modelos numéricos da evolução da paisagem Amazônica, complexidades da evolução de paisagem quando associados à contrastes de resistência litológica e feições transientes da paisagem.

1.5.2 Análises quantitativas

Para explorar o estado e a gênese da transiência da paisagem no Escudo das Guianas, utilizamos dados de relief, perfis longitudinais em espaço χ-z (*chi-plots*), quebras nos perfis longitudinais (*knickpoints*) e índice de declividade do canal normalizado (k_{sn}) através das ferramentas Topographic Analysis Kit (TAK; Forte & Whipple, 2019) e Topotoolbox (Schwanghart & Scherler, 2014). Para isto, utilizamos o Modelo Digital de Elevação (DEM) extraído do Shuttle Radar Topography Mission (SRTM GL3) Global de 90 m pelo website Open Topography: NASA Shuttle Radar Topography Mission (SRTM) (2013). Esta resolução foi escolhida para reduzir o tempo de processamento dos dados devido à grande extensão da área de estudo, que abrange 4° x 4° graus de latitude e longitude. Para explorar os efeitos litológicos, utilizamos a base de dados geológicos do Serviço Geológico do Brasil, com escala 1:1.000.000 (Geobank, CPRM). A seguir, explicamos a obtenção de dados e o propósito da análise de cada métrica utilizada neste estudo.

Os métodos utilizados para analisar a paisagem do Escudo das Guinas revelam estados transientes da paisagem. Análise de *relief* (ver Seção 3.3.1), pode revelar padrões espaciais que indicam transiência da paisagem consistentes com quedas do nível de base, pulsos erosivos e variação na resistência litológica (Ahnert, 1970). Além disso, é possível prever a direção de migração dos divisores de drenagem por meio da análise de *relief* assimétrico entre os divisores.

Outro método utilizado é o mapeamento de feições anômalas da paisagem indicando eventos de captura de drenagem e vales de drenagem abandonados (*wind-gaps*) (ver Seção 3.3.2). Capturas de drenagem de grande magnitude são capazes de "roubar" bacias inteiras de cima do platô do Escudo das Guianas, gerando pulsos erosivos e modificando a configuração da rede de drenagem (Crosby and Whipple, 2006; Whipple and Tucker, 1999). Já capturas de drenagem menores, mais comuns em bordas de platôs e regiões próximas à divisores de drenagens causam recuos graduais/progressivos da escarpa e do divisor de drenagem (Bishop, 1995).

Análise do índice do canal normalizado (K_{sn}) (ver Seção 3.3.2) permite distinguir variações espaciais nas taxas de erosão, importantes para identificar pulsos erosivos em bacias de drenagem e litologias com diferente eficiência erosiva. No caso de rochas mais resistentes o k_{sn} terá altos valores e apresentará baixa eficiência erosiva e vice-versa (e.g. Forte *et al*., 2016).

Neste estudo, utilizamos *chi-plots* para analisar os padrões de k_{sn} e a presença de *knickpoints* consistentes com quedas do nível de base (ver Seção 3.3.4, 3.3.5). Uma forma de analisar a paisagem no *chi-plot,* ou desequilíbrio da paisagem, é através da presença de inflexões, ou desalinhamento do perfil do rio (Whipple and Tucker, 1999). Eventos de queda de nível de base e processos de captura geram padrões sistemáticos no *chi-plots.* Se um mesmo evento de queda de nível de base ocorreu na área de estudo, knickpoints em valores de mesma elevação serão encontrados em todas as bacias. Se houver processos de queda de nível de base combinado com efeito litológico, o *chi-plots* irá plotar *knickpoints* com valores iguais em elevação, porém em diferentes valores χ.

Por último, quedas no nível de base geram *knickpoints* que se propagam a montante proporcionalmente à potência erosiva do canal (e.g. Crosby and Whipple, 2006). Dados empíricos e teóricos sugerem que, uma vez gerados, *knickpoints* se propagam a velocidades de em função da área da bacia de drenagem e da eficiência erosiva.

Com o intuito de compreender a dinâmica da rede fluvial no platô do Escudo das Guianas, utilizamos os métodos citados acima para entender melhor o estado transiente da paisagem e os padrões de reorganização da rede de drenagem.

1.6 ESTRUTURA DA DISSERTAÇÃO

A dissertação é apresentada na forma de artigo científico de acordo com as normas do Programa de Pós-Graduação em Evolução Crustal e Recursos Naturais da Universidade Federal de Ouro Preto. A dissertação está estruturada da seguinte forma:

Capítulo 1: Descreve a natureza do problema, localização da área de estudo e um resumo da metodologia utilizada.

Capítulo 2: Apresenta o manuscrito "***Ongoing landscape transience in the Eastern Amazon Craton consistent with lithologic control of base level***", submetido ao *Earth Surface Processes and Landforms Journal*. Este trabalho apresenta um estudo detalhado da geomorfologia, litologia, e interpretações da evolução da paisagem na área de estudo, NE do Escudo das Guianas.

Capítulo 3: Trata das considerações finais do trabalho e implicações para futuras investigações de paisagens pós-orogênicas

Apêndice: Contém informações suplementares que fornecem análises sobre os parâmetros usados na geração dos resultados.

CAPÍTULO 2

ONGOING LANDSCAPE TRANSIENCE IN THE EASTERN AMAZON CRATON CONSISTENT WITH LITHOLOGIC CONTROL OF BASE LEVEL

Camila M. Fadul[1]*, Pedro Val[1]

[1] Programa de Pós-Graduação em Evolução Crustal e Recursos Naturais, Departamento de Geologia, Escola de Minas, Universidade Federal de Ouro Preto, Morro do Cruzeiro, 35400-000, Ouro Preto, MG, Brazil, fadulcm@gmail.com

This article was sumitted to Earth Surface Processes and Landforms Journal

ABSTRACT

Geomorphic features such as drainage captures, knickpoints, paleochannels, and wind-gaps have long been observed in the Amazon region and typically thought to result from climate change and intraplate tectonics. The influence of rock type as a trigger of these landscape transients is largely overlooked. In the eastern Guiana Shield of the Amazon Craton, shield rivers cross over to the sedimentary rocks of the Amazon basin across a sharp lithologic transition before their confluence with the Amazon River. The transition in rock type is marked by an expressive Main Escarpment (ME) formed over highly resistant sandstones of the basal units of the Amazon Sedimentary Basin. Here, systematic patterns of divide migration and river captures are observed and provide a natural laboratory to study the influence of rock type in landscape transience in a cratonic setting. Through quantitative geomorphology analysis of relief, chi-plots, knickpoints, and river steepness, we investigate if this sharp lithologic transition contributed to the observed patterns of drainage rearrangement. The results revealed that rivers of larger drainage areas flowing across shorter lengths over the resistant rocks of the ME systematically capture neighboring basins. We argue that, as base level fall of the Amazon River migrates upstream into its tributaries draining the shield, they are differentially slowed down by the resistant rocks, generating a series of transients such as drainage capture, divide migration and disparity between the distances traveled by knickpoints. The widespread and systematic features suggest this could be an important autogenic mechanism controlling drainage network rearrangement in the Amazon region as well as other post-orogenic landscapes. The protracted exhumation of resistant rocks in cratons and continent interiors may keep landscapes in perpetual disequilibrium depending on their lithological complexity and offer an exceptional natural laboratory to study landscape dynamics associated with rock type.

Keywords: landscape transience, wind-gaps, knickpoints, lithologic control, Amazon, cratonic landscape

2.1 INTRODUCTION

The presence of knickpoints in river basins is most commonly thought to reflect the upstream propagation of a change in base level triggered by wholesale landscape uplift or base level fall, the latter of which may have a tectonic or climatic trigger (e.g. Rosenbloom and Anderson, 1994; Whipple and Tucker, 1999; Crosby and Whipple, 2006; Gallen *et al*., 2011). However, this typical view of a monotonic upstream propagation of knickpoints is not simple in regions with heterogeneous bedrock lithology, a common feature of large river basins in continent interiors. Local erodibility contrasts along rivers control the upstream knickpoint migration rate and, therefore, the landscape response time to base level perturbations (e.g. Harbor *et al*., 2005; Berlin and Anderson 2007). Importantly, the localized exhumation of resistant rocks can lead to differential knickpoint migration rates and response times among neighboring basins responding to the same change in base level (Harbor *et al*., 2005; Forte *et al*., 2016; Perne *et al*., 2017; Wolpert and Forte, 2021). Under such scenarios, lithological complexity may trigger the migration of drainage divides and river reorganization in neighboring basins that otherwise would not change shape (Bernard *et al*., 2021).

In the Amazon region, the presence of knickpoints and other transient landscape features is most commonly interpreted to reflect intraplate tectonism (Val *et al*., 2014; Rossetti *et al*., 2015), climate change (Irion *et al*., 2009; Pupim *et al*., 2019; Albuquerque *et al*., 2020), and large-scale continental tilting due to mantle and flexural warping of the upper crust (Shephard *et al*., 2010; Sacek, 2014; Bicudo *et al*., 2020). Though largely overlooked in the Amazon region, spatially variable bedrock lithology is known to cause long-lasting river reorganizations in tectonically stable, post-orogenic settings (e.g. Gallen, 2018). In tropical lowland regions, the influence of bedrock resistance to erosion on the landscape evolution is, at best, invoked to explain the formation of highly resistant lateritic duricrusts and long-lasting paleosurfaces or pediplains (e.g. Théveniaut and Freyssinet, 1999; Allard *et al*., 2018; Guillocheau *et al*., 2018). However, about half of the Amazon region is situated over cratonic terranes with complex lithologic distribution and not necessarily covered by lateritic crusts. Lithologic complexity may play an important, but underestimated role in the current configuration of large tributaries of the Amazon River through its influence on the transmittance of changes in base level downstream.

In this study, we challenge the long-held perception that lowland landscapes such as those of the Amazon region are perturbed mostly by intraplate tectonics or climatic change and are otherwise static. We demonstrate that base level fall in the Amazon River triggered ongoing landscape

transience resulting in complex topographic patterns with sharp topographic escarpments, asymmetric drainage divides, river captures, knickpoints, and steep river reach transitions which resemble that of erosive pulses (Fig. 2.1A-B). We argue these geomorphic features are consistent with upstream migrating knickpoints and drainage divide migration in the eastern Guiana Shield controlled by the spatially complex bedrock distribution (Fig. 2.1C). The results presented herein have important implications for the evolution of drainage network patterns in the Amazon region and post-orogenic landscapes in general.

2.2 LITERATURE REVIEW

2.2.1. Geologic evolution and base level history of the study area

The Guiana Shield is the surface expression of the northern half of the Amazon Craton. Its rock substrate formed in the Archean-Proterozoic Eras (3 - 2.5 Ga) with the amalgamation of terrains that formed the Amazon Craton (e.g. Cordani and Teixeira, 2007). At the beginning of the Paleozoic Era (541 Ma) an east-west striking extension developed in the middle of the craton and created the accommodation space for the Paleozoic sedimentary basins, separating it into north (Guiana Shield) and south (Brazilian Shield) portions (Wanderley-Filho *et al*., 2010). Today, this contact outcrops north of the lower Amazon River (Fig. 2.1C).

The opening of the South Atlantic Ocean during the Cretaceous (135 to 110 Ma) culminated in the formation of the South American northeast coast and the mouth of the Amazon River in its current position (Wanderley-Filho *et al*., 2010). This newly formed mouth in the Atlantic Ocean was likely accompanied by base level fall and an erosive wave in the eastern Amazon region, which so far was disconnected from the western Amazon region (Figueiredo *et al*., 2009). The western (West Amazon basin) and eastern (proto-Amazon basin) portions of the Amazon drainage networks had their drainage divide near the modern Negro-Solimões river confluence (~200 km west of the study area) and connected ca. 9.4-9 Ma to form the transcontinental Amazon River (Hoorn *et al*., 2010; Hoorn *et al*., 2017). The integration of the western basin to the eastern Amazon doubled the eastern basin's drainage area, likely readjusting the equilibrium profile of the eastern proto-Amazon river and driving excavation of the lower reach. From the late Miocene until the present times, successive events such as accelerated uplift of the Andes and climate change (including Pleistocene glaciations) possibly resulted in higher erosion rates, increased water supply, and sediment flow along the entire Amazon River (Figueiredo *et al*., 2009; Gorini *et al*., 2013; Hoorn *et al*., 2017; Boschmann, 2021), which may also have contributed to the excavation of the lower Amazon riverbed. The integrated history of base level changes in the Amazon river, therefore, is likely to have generated multiple perturbations in its main tributaries, including those in the Guiana Shield.

2.2.2 Timing of paleosurface formation and erosion rates from lateritic covers

Lateritic surfaces are typically resistant to erosion. Close to- or in the study area, laterites are located (1) in Suriname and French Guiana in elevations of 75 to 400 m (north of the plateau) (Théveniaut and Freyssinet, 1999; Aleva, 1981), (2) in the Jari River basin (Aleva , 1981) between 200 to 600 m (Basin 8, Fig. 2.1), (3) near the mouth of the Rio Trombetas over the Alter do Chão Fm. (Cretaceous-Paleogene) at altitudes of 100 to 200 m (Grubb, 1979; Aleva, 1981; Costa *et al*., 2014) (Lateritic cover on 57°W, 2°S - Fig. 2.1A, C) and (4) 200 km along-strike to the west of the study area, also over the Alter do Chão Fm. (Balan *et al*., 2005; Peixoto *et al*., 2009; Costa *et al*., 2014). Laterites are typically elevated from the local base level and mark a transition from an erosive lull to an excavation event, forming dissected table-top surfaces (e.g. Théveniaut and Freyssinet, 1999; Balan *et al*., 2005).

Despite occurring in distinct regions throughout the Amazon, lateritic profiles are coeval and correspond to paleoclimatic variations throughout the Cenozoic (Allard *et al*., 2018). There are at least three periods of formation of lateritic profiles in the Amazon region. Paleomagnetic studies in Suriname and French Guiana revealed several lateritization ages between 80 to 10 Ma, the most recent age being 2 Ma (Théveniaut and Freyssinet, 2002), consistent with U-Th/He ages of bauxite, lateritic, and manganese duricrusts elsewhere in the Amazon region (Allard *et al*., 2018; Albuquerque *et al*, 2020). In the study area (Fig. 2.1A, C), the laterites developed at the mouth of the Rio Trombetas, Rio Paru and Rio Jari do not have constrained ages (e.g. Costa *et al*., 2014). However, the geological context is the same as the laterites near Manaus (west of the study area along-strike), where ages of 25 Ma, 14-11 Ma and 9-6 Ma have been reported (Balan *et al*., 2005). Therefore, the ages of lateritic surfaces mentioned above may have regional correspondence.

The elevation-age ratio of lateritic surfaces in or close to the Guiana Shield suggests excavation rates in the order of 2 to 25 m/Ma in the last 10 Ma (Théveniaut and Freyssinet, 1999; Théveniaut and Freyssinet, 2002; Balan *et al*., 2005; Allard *et al*., 2018). These rates agree with the millennial erosion rates of 10 to 40 m/Ma obtained from cosmogenic isotopes in the Amazon craton (Wittmann *et al*., 2011). These studies suggest that the table-top surfaces developed on the Amazon Basin sedimentary rocks in the study area attest to a continuous lowering of the Amazon River base level since the Miocene (Dobson *et al*., 2001; Figueiredo *et al*., 2009; Gorini *et al*., 2013; Hoorn *et al*., 2017; van Soelen *et al*., 2017). This work investigates the transient features of the landscape of the Guianas Shield resulting from this protracted fluvial excavation (Fig. 2.1).

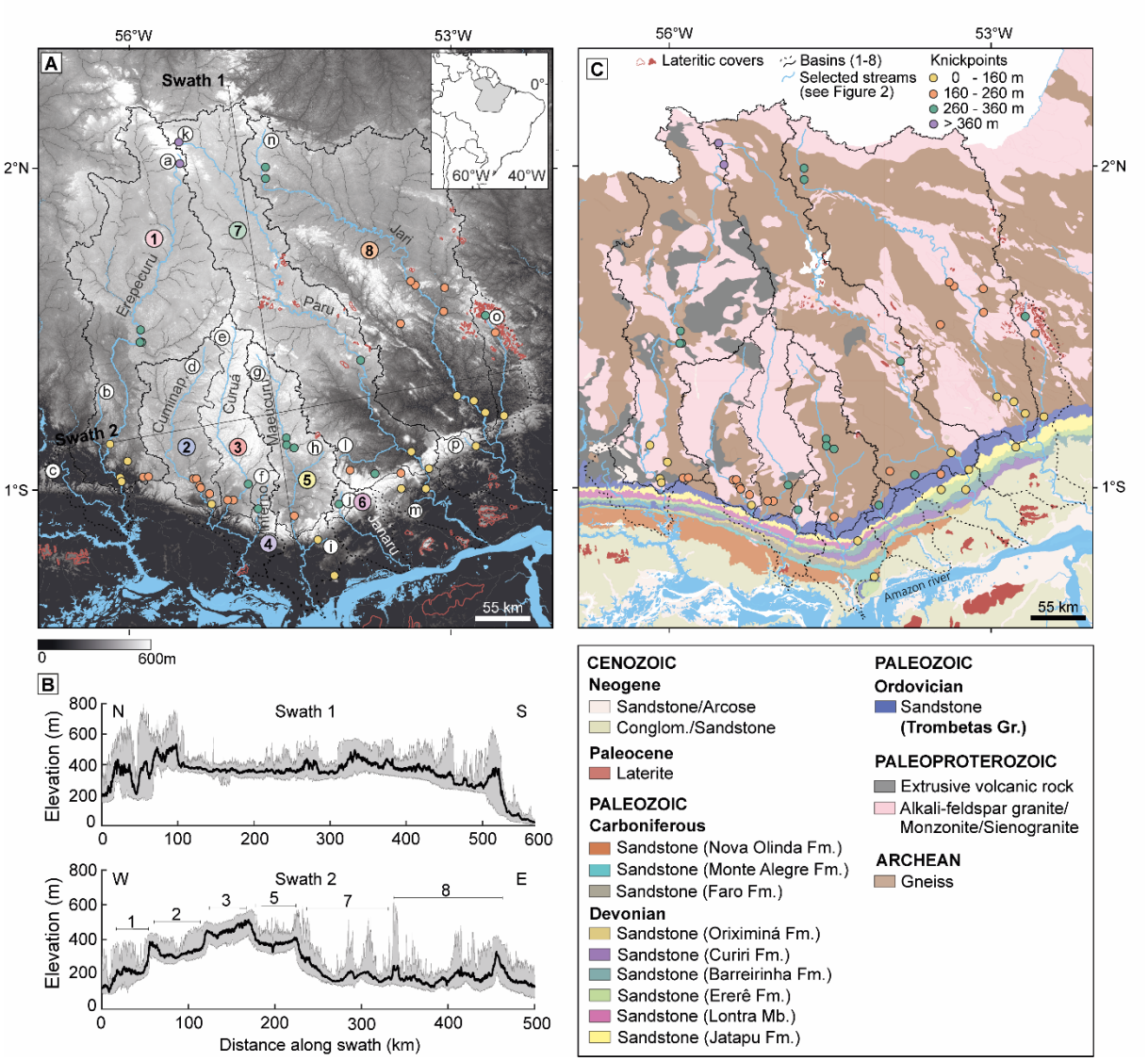

Figure 2.1- Topography and geology of eastern Guiana Shield. A) Topographic map of the Eastern of Guiana Shield. The main river basins analyzed in this work: 1 – Erepecuru R.; 2 – Cuminapanema R.; 3 – Curuá R.; 4 – Inferno R.; 5 – Maecuru R.; 6 – Janaru R.; 7 – Paru R.; 8 – Jari R. Circles of various colors show the location of 50 knickpoints automatically extracted from the DEM. Solid outlines show basins pinned to the downstream limit of the resistant rocks of the Trombetas Gr. Dashed lines show the basin outlines down to the confluence with the Amazon River. B) Swath-profiles across the study area: (1) N-S and (2) W-E indicated by black lines on the topographic map. C) Simplified geologic map of the study area (Brazilian Geological Survey - CPRM). Note locations of mapped lateritic surfaces (dark red polygons in C, red outlines in A). The Ordovician sandstones constitute the Trombetas Gr.

2.3 METHODOLOGY AND METHODS

To explore the state and trigger of landscape transience in the Guiana Shield, we used a Digital Elevation Model (DEM) to extract relief, longitudinal profiles in χ-z space (chi-plots), breaks in longitudinal profiles (knickpoints) and normalized channel slope index (k_{sn}) through the Topographic Analysis Kit (TAK; Forte & Whipple, 2019) and Topotoolbox (Schwanghart and Scherler, 2014) tools. We used the 90 m Global Shuttle Radar Topography Mission (SRTM GL3)

DEM obtained from Open Topography (Farr *et al*., 2007). This resolution was chosen to reduce data processing time due to the large extension of the study area (4° x 4° degrees latitude/ longitude). To explore the lithological effects, we used the geological database of the Geological Survey of Brazil, with a scale of 1:1,000,000 (Geobank, CPRM).

2.3.1 Relief analysis

Absent covariance with lithologic types, relief gradients can reveal uplift gradients and/or changes in base level (Ahnert, 1970). The history of base level fall in the study area (see Section 2.2.1) would increase relief in the lower reaches (e.g. southern portion) which would propagate in the form of erosive waves towards the north of the plateau given the N-S orientation of the river basins (Fig. 2.1). Relief is also a metric that correlates with the resistance of rocks to erosion, i.e. more resistant rocks have higher relief and vice versa (Forte *et al*., 2016). In this study, we compute relief as the mean of the local topographic range within a 2500 m moving window using Topotoolbox (Schwanghart & Scherler, 2014). Using the relief map, we searched for spatial patterns that could indicate landscape transience consistent with changes in base level.

The asymmetric relief distribution on opposite sides of drainage divides constitutes a diagnostic feature of drainage divide migration. The steeper (or lower elevation) side of the drainage divide has greater erosion rate and advances over the less steep (or higher elevation) side, causing migration of the drainage divide (Whipple *et al*., 2017). In this study, we used relief contrasts from opposite sides of drainage divides to qualitatively infer the direction of migration of drainage divides.

2.3.2 Identification of river captures

River captures leave anomalies in the drainage network such as sharp 90° bends (capture elbows), abandoned drainage valleys, wind-gaps with low-elevation divides, drainage divide jumps, and knickpoints in the point of capture (Bishop, 1995). Large magnitude drainage captures can occur when the escarpments separating a plateau from the neighboring plains meet near higher order channels on top of the plateau. In these cases, rivers that drain the escarpment "steal" entire basins from above the plateau, causing erosive pulses that evolve as a base-level fall. Thus, drainage basins that flow over plateaus are especially vulnerable to large captures (e.g. Prince *et al*, 2011; Gallen, 2018). Minor drainage captures also occur at the edges of plateaus, where the headwaters of rivers on the plateau are captured to neighboring basins at lower topographic elevations, causing progressive retreat of the scarp and drainage divide (Bishop, 1995). In this study, we seek evidence of these two types of drainage captures and drainage network reorganization based on relief analysis (see Section 2.3.1), drainage anomalies, river steepness, chi-plots and knickpoint distribution (see Sections 2.3.3

and 2.3.4).

2.3.3 River steepness (k_{sn}) analysis

We computed and interpreted longitudinal river profiles and knickpoints patterns based on the predictions of the stream power model of river incision (Whipple and Tucker, 1999):

$$E = KA^m S^n \quad (1)$$

where E is the fluvial incision rate (m/year), K the erosional efficiency (m[1 – 2m]/year), A the drainage area (m2), S the fluvial gradient (m/m), and m and n are exponents that related to the types of erosive processes that govern bedrock excavation (Whipple, 2001). In equilibrium, Equation 1 predicts that changes in the local gradient of channels describe a negative power-law relationship with the drainage area and with the erosional efficiency:

$$S = (E/K)^{1/n} A^{-m/n} \quad (2)$$

where m/n is the concavity of the river channel, also known as θ. Equation 2 can be observed empirically in bedrock rivers (S = ks A-θ) (Flint, 1974). The term in parentheses in Equation 2 is steepness index (k_s) and depends on the value of θ. For a fixed θ, k_s is referred to as the normalized steepness index (k_{sn}). In case of more resistant rocks (i.e. low erosional efficiency), k_{sn} will be high and vice-versa (e.g. Forte *et al*., 2016). In the absence of lithological variations, spatial patterns of k_{sn} can be interpreted as variations in erosion rates and, therefore, are useful to identify erosive pulses in drainage basins. In this study, we generate a map of k_{sn} calculated through automated regressions following Equation 2 (θ = 0.45, see Section 2.3.4) on smoothed profile data with a 1000 m window without distinguishing confluences between main and tributary rivers (e.g. quick method in TAK; Forte and Whipple, 2019).

2.3.4 Chi-Elevation analysis and paleo profile reconstruction

Equation 2 implies that elevation variations along the longitudinal profile of a channel depend on variations in erosion rate (or uplift), rock type, and drainage area. This is evident in the integral solution of Equation 2 (Perron and Royden, 2013):

$$z = z_b + (E/K)^{\frac{1}{n}} \int_{x_b}^{x} \left(1 / A(x)^{\frac{m}{n}} \right) dx \quad (3)$$

where zb is the elevation at the assumed base level (xb) and x is the along-channel distance from base level. The integral term in Equation 3 is known as χ and can be calculated directly from the flow accumulation grid obtained with a DEM. Note that Equation 3 describes a straight line when the landscape is in equilibrium with a slope equal to k_{sn} and any inflection in a plot of z vs χ (known as

chi-plot) denotes changes in E or K (Perron and Royden, 2013).

Drainage captures alter the pattern of drainage area and can lead to local inflections (i.e. knickpoints) in the chi-plots and disturb the collinearity between neighboring basins even if they drain to the same base level (Willett *et al*., 2014; Giachetta and Willett, 2018). Base level falls also generate knickpoints that separate a smooth portion upstream of the inflection (relict area) from a steep zone (adjusted area) that transmits the base level fall signal in the form of upstream propagating waves (Whipple and Tucker, 1999; Crosby and Whipple, 2006). Continuous lithological contacts can also generate inflections like those of base level fall, but these knickpoints are fixed at lithological contact (Whipple *et al*., 2013; Wolpert and Forte, 2021).

We used chi-plots to study k_{sn} patterns and the presence of knickpoints consistent with base level fall. In the 8 basins studied here, we applied an optimization function to the portions of river channels upstream of a local base level inferred at the contact between the shield and sedimentary basin rocks (Schwanghart and Scherler, 2014). The best-fit theta varied between 0.3 and 0.7, consistent with the window of values for bedrock rivers (Whipple *et al*., 2013), but a relatively large range to work with. Therefore, we use the value of 0.45 as it fits into this range and is a widely used value in the literature. For reference, we provide chi-plots with θ values between 0.3 and 0.6 and constrained θ values for all basins in the supplemental material (Supplementary Figure S1 and Table S1).

Chi-plots were produced for the main channels and selected tributaries of the studied basins (lowercase letters a – q in Fig. 2.1A and 2.5). The chi-plots were generated using a constrained regularized smoothing function (i.e. crs routine, Topotoolbox) with tau and K values of 0.1 and 1 respectively, and used to automatically identify knickpoints (Schwanghart and Scherler, 2014; 2017). For the latter, we used a topographic-step tolerance of 30 meters based on a noise-magnitude identification routine as follows: the DEM was first hydrologically corrected by imposing elevation minima through positive peaks in the along-stream noise (i.e. carving) and by infilling the valleys through the same noise (i.e. filling). The noise distribution resulting from their difference revealed that 30 m is higher than most observed errors (Fig. 2.2) and yield knickpoints in consistent inflections in the chi-plots (see Results). Lithological and base level controls on the positions of knickpoints were then carefully assessed for each stream profile and considering all basins in concert.

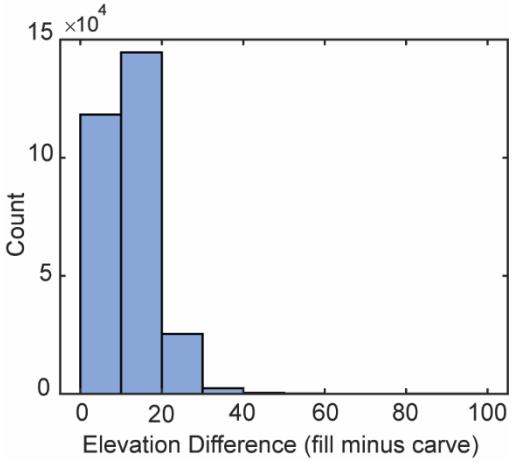

Figure 2.2- Topographic uncertainty histogram of the Digital Elevation Model used in this study. A maximum error of 70 m was identified, but we note that the majority of errors is below 30 m, which is the tolerance value used to automatically map knickpoints.

To reconstruct the relict portions of rivers in the Guiana Shield, we used the chi-plots to select reaches upstream of knickpoints which are not associated with lithological contacts. We applied a linear regression on the interpreted relict stretch in chi-z space to obtain the coefficients of Equation 3 using TAK (Forte and Whipple, 2018). The profiles were projected from the relict stretch to the topographic escarpment supported by the rocks of the Trombetas Gr. (see Fig. 2.1). We restricted the projection to this portion as the rocks in this group (mostly sandstones) are highly resistant to erosion and locally control the base level.

2.3.5 Knickpoint analysis and interpretation

Base level falls generate knickpoints that propagate upstream in proportion to the channel's erosive power (e.g. Crosby and Whipple, 2006). Empirical and theoretical data suggest that, once generated, knickpoints propagate at horizontal velocities (Vkp) governed by Am and K and are typically linearly proportional to the slope (dz/dx), that is, n = 1 in Equation 1 (Lague, 2014), generating:

$$V_{kp} = KA^m \quad (4)$$

In the study area, catchments 1 through 8 have different drainage areas and systematic patterns of knickpoints, drainage captures, and along-strike elevation (see Results). Here, these differences are interpreted in terms of Equation 4.

2.4 RESULTS

2.4.1 Relief analyses

The northern half of the plateau (i.e. south of ~1° N) contains lower relief compared to the southern half (Fig. 2.3A, also evident in Fig. 2.1B). The Guiana Shield-Amazon Sedimentary Basin contact, henceforth referred to as shield-lowland transition, is marked by a continuous curvilinear topographic escarpment extending approximately E-W (Fig. 2.1B; 2.3A). This topographic feature, henceforth referred to as the main escarpment (ME), contains high relief on both northern and southern flanks as well as flat tops coincident with the resistant sandstones of the Trombetas Gr. (Fig. 2.1).

South of the ME, relief is mostly <100 m but contains local, high relief zones coincident with variable lithology, especially at the edges of local tabletop surfaces supported by lateritic duricrusts to the east (compare Fig. 2.1C and 2.3A). Immediately north of the ME, we identify low-relief zones coincident with the lowest plateau elevations within each basin (Fig. 2.1A, B and 2.3A). Basins 7 and 8 are particularly noteworthy for the semi-circular format of this low-relief zone (Fig. 2.3A). In their upstream limit, the low-relief zones are marked by knickpoints (Fig. 2.1A, B, Fig. 2.3; see also Section 2.4.2) and are sometimes coincident with topographic escarpments with high relief (e.g. box E in Fig. 2.3A).

Drainage divides in the outer limits of the plateau are asymmetric. This pattern repeats itself on the plateau as well, e.g. basins 2, 3 and 5 have low relief near the respective drainage divides but are surrounded by higher relief within the neighboring basins (Fig. 2.3A). Overall, the relief at the divide going from the outer edges of the plateau (e.g. basins 1 and 8) towards the next basin over (plateau-ward) is systematically lower.

The asymmetric divides revealed in the relief map are ripe with evidence of topographic transience such as river captures and wind-gaps (Fig. 2.3B-H). At the western edge of the plateau (Basin 1), upland rivers flow southward consistent with the main flow direction of the plateau. Rivers closest to the edges are captured by lowland rivers and make anomalous 90° westward turns (i.e. capture elbows; Fig. 2.3B-D). Coincident with the river captures in the headwaters of Basin 1 are anomalous patterns of drainage divides, which have locally retreated southeastward (Fig. 2.3B). We also infer at least three other capture events within the plateau where basins 3, 5, and 8 captured basins 4, 6, and 7 respectively. The capture of basin 4 by basin 3 is suggested by the presence of an anomalous SW turn coincident with a knickpoint in the middle portion of basin 3 (Fig. 2.3E). Here, the divide is located over a low relief region (Fig. 2.3A). An increase in k_{sn} immediately upstream of this knickpoint is also observed (Fig. 2.4A; see Section 2.4.2). The capture of basin 6 by basin 5 is

suggested by 180° turns of rivers close to the divide with basin 6, as well as its low elevation and relief (Fig. 2.3A). The capture of Basin 7 by Basin 8 is also suggested near the headwaters in the northern portion of the plateau (Fig. 2.3A, G), also associated with anomalous river turns and an inferred drainage divide retreat based on relief asymmetry (Fig. 2.3G, H).

Lastly, we identified abandoned valleys all along the ME located near or at the drainage divide in a higher elevation than the valleys formed by the modern main rivers. The clearest example is a wind-gap located westward of the Parú River in Basin 7 (Fig. 2.3F). Other examples are detailed in Section 2.4.4.

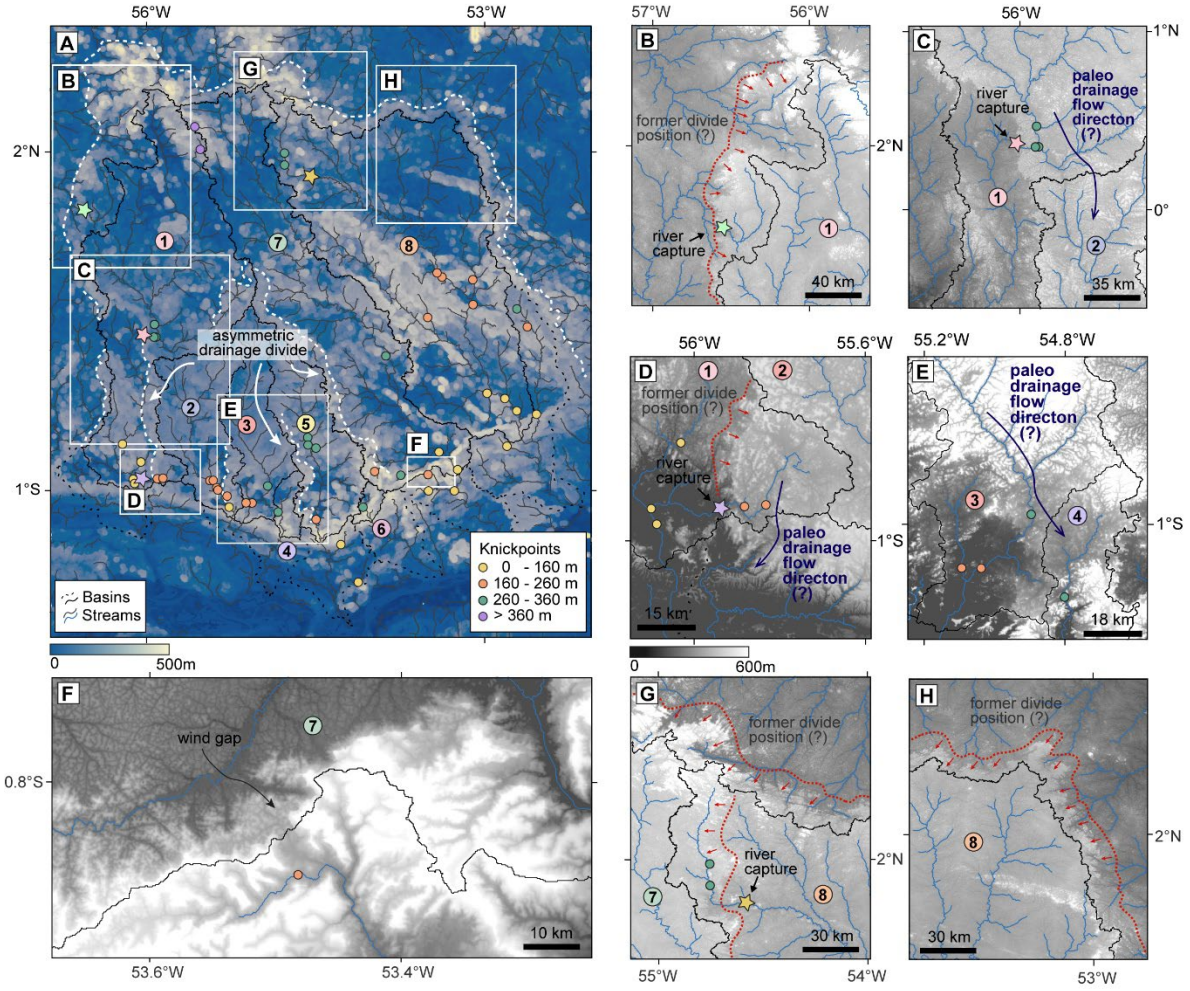

Figure 2.3- Geomorphic evidence of river capture and divide migration. A) Local relief map showing knickpoints (circles) and location of detailed views in panels B-H. B) Anomalous pattern of the drainage divide (solid black line) and interpreted position of the paleodivide location (dotted red line) and southeastward migration direction induced by river capture (red arrows). Also shown are the location of a river capture (green star) and a capture elbow. C) Major river capture of upland plateau drainage (former half of Basin 2) by the Erepecuru River (trunk stream of Basin 1). D) Retreated position of the main drainage divide (solid black line) between basins 1 and 2 with respect to the topographic escarpment (dotted red line) indicating another river capture (purple star). E) Anomalous SW turn in the Basin 3 trunk stream coincident with a knickpoint and the upstream limit of Basin 3's low-relief patch. Arrows indicate a possible paleoflow connecting the area upstream of the knickpoint to Basin 4 through a low-relief drainage divide. F) Wind-gap located on the ME

indicative of a barrier-crossing paleo river with southward flow. G) River capture (yellow star) in the headwater of Basin 7 by Basin 8; H) Drainage divide asymmetry in the northeastern limit of Basin 8. Divide-parallel escarpments with high relief suggest westward retreat of the divide (red arrows).

2.4.2 River steepness: spatial patterns

The regional pattern of k_{sn} agrees with the relief patterns. The highest steepness values are coincident with the ME and the Trombetas Gr. rocks, as expected for highly resistant lithology (Fig. 2.4). The most frequent values are low (0 - 10 m0.9), consistent with a cratonic environment. Higher values of k_{sn} are also observed in isolated segments of some main channels or tributaries of the studied basins (Fig. 2.4A). Intermediate to high values of k_{sn} (20 - 40 m0.9) also mark the high-relief regions at the outer edges of the plateau compared to neighboring basins that have headwaters on the plateau (Fig. 2.4A). More specifically, the eastern outer edge, in the headwaters of the basins that drain into the Atlantic Ocean have higher k_{sn} values than the headwaters of Basin 8 to the west. To the east where lithologic maps are available, the patterns do not coincide with a change in lithology (Fig. 2.4B).

The drainage divide that separates basins 5, 6 and 7 has high k_{sn} contrasts, with Basin 7 having steeper rivers. We interpret this pattern as an asymmetry along this divide suggesting westward migration, in agreement with the relief data (Fig. 2.4A). We also observe k_{sn} asymmetry around the divide between basins 7 and 8, Basin 8 being steeper than Basin 7 near the divide, also suggesting westward migration (Fig. 2.4A). Lastly, asymmetric k_{sn} values near divides do not seem to change systematically with lithology, except for the areas surrounding lateritic covers and some NW-SE trending metamorphic rocks in Basin 8, where we also observe high k_{sn} (> 40 m0.9).

On the plateau, k_{sn} values are mostly low (< 10 m0.9) from the middle to the upper course of basins 1, 7 and 8. However, basins 5, 7 and 8 have a radially shaped high k_{sn} zone not systematically coincident with changes in lithology (Fig. 2.4). We also observe an intermediate k_{sn} zone in the middle to lower course of all basins, albeit not as systematic as in basins 5, 7, and 8. In basin 3, this zone is immediately upstream of the anomalous turn interpreted as a possible location of river capture (see Fig. 2.3E) but also coincident with a change in lithology (Fig. 2.4). Nonetheless, this lithology is the same granitic rock as in other basins and, therefore, likely is not the cause for the locally high steepness. The zones of high k_{sn} do not systematically coincide with lithological variations, except for Basin 8 (Fig. 2.4B). Lastly, basins 3 and 5 have higher k_{sn} values distributed in tributaries throughout the basin, which does not occur in neighboring basins. This pattern is clearer in chi-plots (see Section 2.4.3).

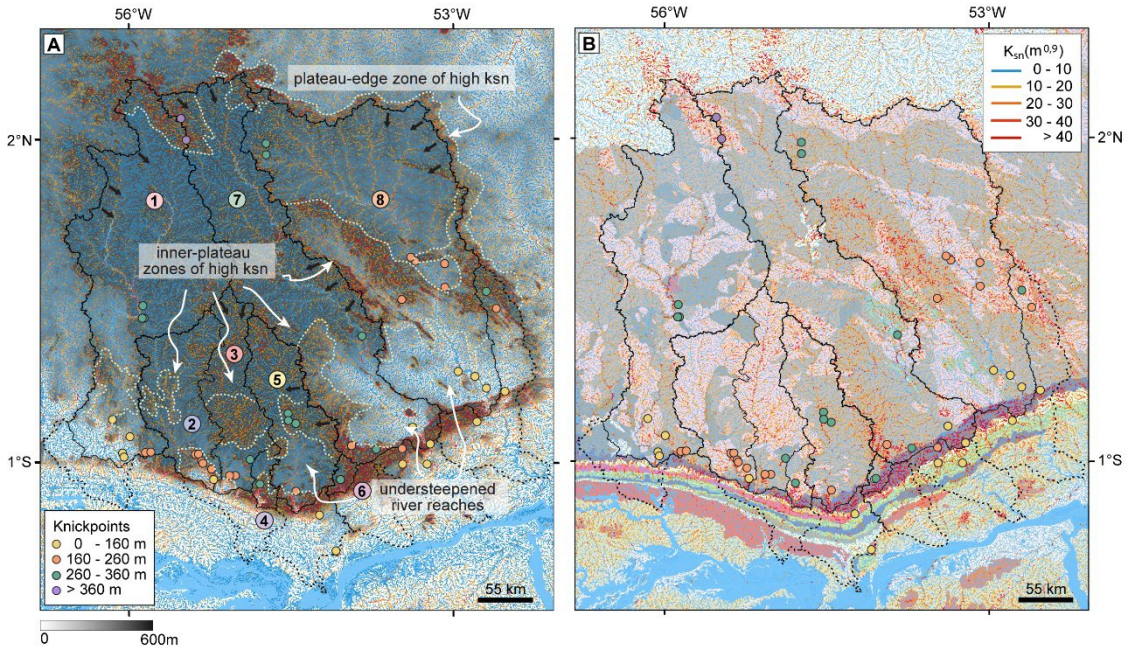

Figure 2.4- k_{sn} map over topography (A) and lithology (B). White dotted lines represent zones with high **k_{sn}** values. Black arrows indicate possible direction of movement of the drainage divides based on the surrounding asymmetric **k_{sn}** values. Shown are knickpoints colored by the most elevation windows of river reach they separate. Geologic map colored as in Fig. 2.1C.

2.4.3 Chi-plots and knickpoints

Chi-plots reveal the existence of 1 to 4 distinct, widely distributed low-slope benches (LSB) of collinear chi-profiles at different altitudes which are separated by knickpoints and steep breaks in the profiles (Fig. 2.5). We observe the following LSBs: (1) 79-125; (2) 180-226 m; (3) 262-336 m; (4) 458-475 m. Despite the LSBs being present in all the studied basins to varying degrees, the slope of the chi-z plot (k_{sn}) of each LSB varies according to the basin's drainage area. For example, LSB 2 in basins 2 and 5 as well as LSB 3 in basins 2-6 have higher k_{sn} than in other basins (compare insets in Fig. 2.5). The k_{sn} of rivers that drain the ME is also lower in Basin 8 than in basins 2-6 (compare blue profiles in Fig. 2.5). Together, this pattern reveals higher k_{sn} (of LSBs and rivers) in the central and southern part of the plateau where the ME-traversing river basins are smallest (Fig. 2.4, 2.5). Interestingly, LSBs in the same basin (i.e. #2 and #3 in Basin 5) have similar k_{sn} and are only separated by a step in the profile (Fig. 2.5C).

LSB 1 is bounded by knickpoints (yellow) at its lower limit with an average of 109 ± 32 m (yellow circles in Fig. 2.5) and occur both on sandstones and granitoids both north and south of the ME: basins 1 (stream c, Fig. 2.5A and Fig. 2.1A), 5 (stream i, Fig. 2.5C), 7 (stream l, Fig. 2.5E) and 8 (stream o, Fig. 2.5F). North of the ME, these knickpoints are always near the shield-lowland transition (Fig. 2.4 and 2.5).

LSB 2 is bounded by knickpoints (orange) near 210 ± 19 m over granitoids of different origins in all basins (orange circles in Fig. 2.5), except for Basin 6. Rivers a (Fig. 2.5A), d (Fig. 2.5B), h (Fig. 2.5C), and n (Fig. 2.5F) are highlighted to illustrate this LSB and flight of knickpoints but many smaller tributaries in these catchments drain this LSB (see Fig. 2.5). These knickpoints are not coincident with the shield-lowland transition. In basins 2 and 3, they are farther north of the ME, clustered in chi-z space, especially in basins 2-4 (Fig. 2.5B), and limit the low k_{sn} zone described in Section 2.4.2 (Fig. 2.4A). The latter collapses towards low values of chi (Fig. 2.5B) due to the large drainage area of the ME-crossing basins. These knickpoints also occur in basins 1 and 7 but are associated with drainage captures, consistent with steps on the chi-plot separating LSBs of similar k_{sn} (Fig. 2.3D and F; insets in Fig. 2.5).

LSB 3 is bounded by knickpoints (green) near 274 ± 79 m in the middle to upper course portion in all basins (green circles in Fig. 2.5), except for Basin 2, whose upper basin was captured by Basin 1 (Fig. 2.3A-C). These knickpoints are almost exclusively on the same granitoid rock throughout the study area (Fig. 2.5). In basins 1 to 5, they are clustered in chi-z space despite being in different channels (Fig. 2.4 and 2.5). In basins 4 and 8, these knickpoints appear in granites and laterites, respectively.

LSB 4 in basins 1 and 7 (northernmost areas of the plateau) is bounded by knickpoints (purple) with average elevations of 466 ± 79 m (purple circles in Fig. 2.5). These knickpoints are near the headwaters in the northern edge of the plateau (Fig. 2.4) and have high k_{sn} coincident with granites of the Mapuera Intrusive Suite (Fig. 2.4). These granites also occur scattered over the plateau, where they do not have associated knickpoints.

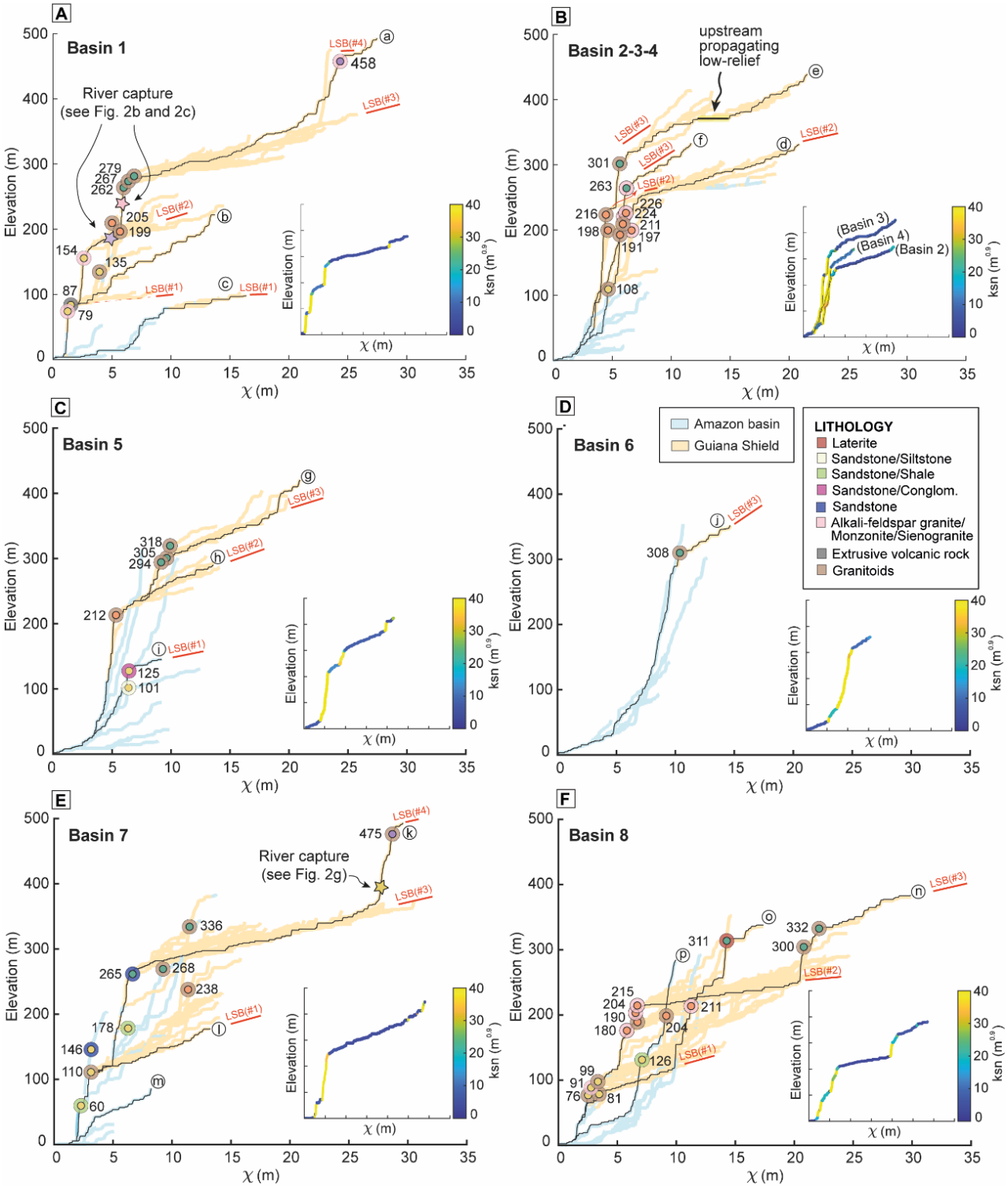

Figure 2.5- Chi-plots of the studied basins showing variations in geological domains (i.e. shield vs lowlands), knickpoints, river captures and ksn. Chi-plots colored by geologic domain (shield and lowland) for studied basins and highlighting selected rivers (black lines with letters a-p; see locations in Fig. 2.1A). Automatically extracted knickpoints and the respective lithologies in which they occur are also shown colored by the range of low-slope benches that they are linked to (see Section 2.4.3). Insets show the trunk streams colored by ksn obtained based on linear regressions in chi-z space. River captures identified in Fig. 2.3 are marked by stars in the chi-profiles. (A-F) Chi-plots for basins 1 through 8.

2.4.4 Excavation of the lower reaches

We identified wind-gap features on top of the ME, which sometimes form part of the drainage divides between the basins that drain the Guiana shield and with headwaters on south-facing slopes of the ME (Fig. 2.6). These wind-gaps are generally oriented north-south, traversing the ME from side to side, and reveal the pre-existence of escarpment-crossing rivers. Wind-gaps occur in the range of ~200 to 270 m along the entire escarpment, that is, elevations similar to the second flight of knickpoints (see Section 2.4.3). The wind-gaps are perched with respect to the nearest escarpment-crossing rivers (left panels in Fig. 2.6B, C, E). The rivers left behind after the formation of the wind-gaps also have knickpoints (e.g. Fig. 2.3F and 2.6A, E), suggesting base level fall which can either be pre- or post-wind-gap formation.

Using Equation 3, we performed a linear regression on the reach upstream of knickpoints in the second and third flights, which we interpret to be related to base level fall. Reconstruction of the Basin 1 trunk stream at the ME (~220 m) coincides with the elevation of a wind-gap (~200 m) located slightly east of it, where other river captures are also evident (Fig. 2.6B). Wind-gaps located east of the Basin 3 outlet (between 7 to 10 km and 12 to 17 km in Fig. 2.6C) with average elevations of ~200 m and ~180 m also match the reconstruction of the Basin 2 trunk stream (~210 m; Fig. 2.6C). Interestingly, the portion of Basin 3 interpreted as captured from Basin 4 (Fig. 2.3E) projects to a higher elevation (~290 m) compared to the lowest wind-gap in this divide, but nonetheless still approximately consistent with the average elevation of the divide (Fig. 2.6C).

Though not a wind-gap, the Basin 6 trunk stream is likely a wind-gap in formation (i.e. a snapshot of the past configuration of the other wind-gaps identified) (Fig. 2.6D). The minimum envelope of Basin 6, located at 18 km, has an elevation of ~200 m coinciding with the elevation of the reconstructed Basin 5 trunk stream and is roughly in agreement with the projection of Basin 6 (shown for reference). Lastly, the wind-gap located west of basin 7 is a remarkable example of a former ME-crossing drainage with a central valley between 9 to 13 km, a width comparable to the modern ME-crossing rivers (Fig. 2.6E), albeit at an average elevation of the minimum envelope ~240 m. Reconstruction of the Basin 7 trunk stream coincides with this wind-gap elevation.

The concordance between projected and wind-gap elevations suggests excavation of the trunk streams, consistent with base level fall. Using the difference between the projected segments and the modern elevation of the river profiles at the downstream end of the modelled reach, we infer incision magnitudes between 161 m (i.e. Basin 6) and 256 m for (i.e. Basin 3). In general, incision magnitudes are similar along the ME.

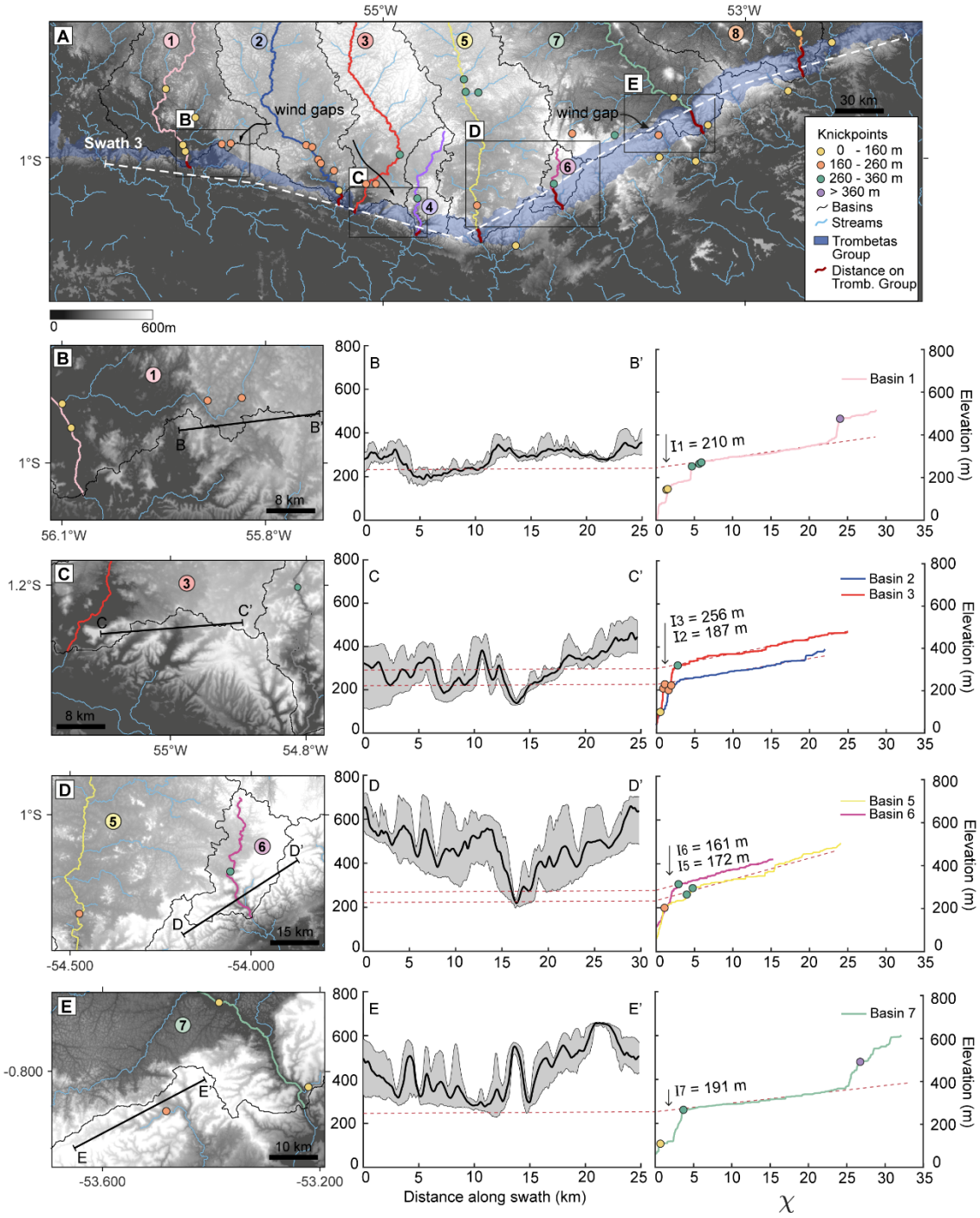

Figure 2.6- Wind-gaps and paleo-profile reconstructions. A) Detailed view of the ME and location of mapped wind-gaps B-E (black boxes). The left panels of examples B-E show the location of the swath profile on the topographic map. The middle panel contains the swath profile of the wind-gap show mean (bold black line) and the maximum and minimum envelope within a 5 km window (the shaded polygon). The right panels show the chi-plot for the selected trunk streams and their reconstruction (red dotted line). The magnitude of incision corresponding to the main rivers of the basins analyzed in this figure is shown by the letter I.

2.4.5 Along-strike trends related to the Main Escarpment

The ME reaches an elevation peak of ~800 m at the approximate medial position of the plateau (~320 km in the profile of Fig. 2.7A). The maximum elevation envelope gradually decreases near-symmetrically towards the west and east, suggesting a near-continuous surface locally dissected by ME-traversing wind-gaps and rivers. In contrast, the average and minimum elevations that have abrupt elevation drops where the main basins traverse the ME but otherwise high mean elevations in between (Fig. 2.7A). This pattern reveals that the excavation of the resistant rocks in the ME is preferential where basins are large enough and have the erosive power to maintain a fluvial connection with the lowlands (Fig. 2.7A). Where ME-traversing channels were abandoned, wind-gaps formed at a relatively small range of elevations (~200 to 300 m) irrespective of along-strike topographic elevations along the ME (Fig. 2.7A). The reconstructed profiles roughly agree with these wind-gap elevations, suggesting that ME-traversing rivers had similar outlet elevations in the past, unlike the modern scenario where outlets vary according to the along-strike topography of the ME (compare minimum elevation envelope in Fig. 2.7A).

In general, the lateritic surfaces located on rocks from the Amazon sedimentary basin have lower elevations and range from 55 to 416 m, with an average of 373 ± 121 m (Fig. 2.7B). The elevations of laterites developed on rocks of the Guiana Shield are higher, ranging from 300 to 600 m, the highest of which occur between basins 7 and 8. Lateritic surfaces south of the ME climb in elevation from west to east (Fig. 2.7B). Interestingly, the second and third flight of knickpoints have elevations similar to the elevation range of the lateritic surfaces south of the ME.

We observe that basins with larger drainage area (Basins 1, 7 and 8) have low average elevations (~280 to 390 m) when compared to basins smaller in area (Basins 2, 3, 4, 5 and 6) (Fig. 2.7C). Larger basins with lower average elevations capture basins with smaller area at higher elevations (Fig. 2.7C). The divide migration direction suggested by the relief and k_{sn} patterns agree with the drainage capture directions observed for basins 1, 2, 5, 7 and 8 (Fig. 2.7C). The pattern of drainage captures and divide migration suggests a systematic longitudinal (i.e. E-W) consumption of the innermost regions of the plateau. Also, basins that flow a shorter distance over the Trombetas Gr. capture drainages from adjacent basins which flow a greater distance in the same rocks (Fig. 2.7D). Thus, basins with long travelled distances over the hard rocks and smaller drainage areas are captured by its neighbors (Fig. 2.7D).

In basins 7 and 8 (eastern boundary), the second and third flight knickpoints (which project to the elevation of wind-gaps) are more than 100 km away from the ME, while corresponding knickpoints in other basins to the west are less than 50 km from the ME (Fig. 2.7E), except for Basin 1 (western limit). Here, the third flight of knickpoints is associated with a drainage capture of the

headwaters of Basin 2 more than 100 km from the ME (Fig. 2.7E, see also Fig. 2.3C and Fig. 2.5). In the central portion of the plateau (Basin 5), the third flight of knickpoints are also distant from the ME (>50 km), consistent with its larger drainage area in relation to neighboring basins (e.g. basins 4 and 6, see Fig. 2.6A and 2.7E). Thus, knickpoints further away from the ME are associated with basins with larger drainage areas as well as drainage captures (Fig. 2.7).

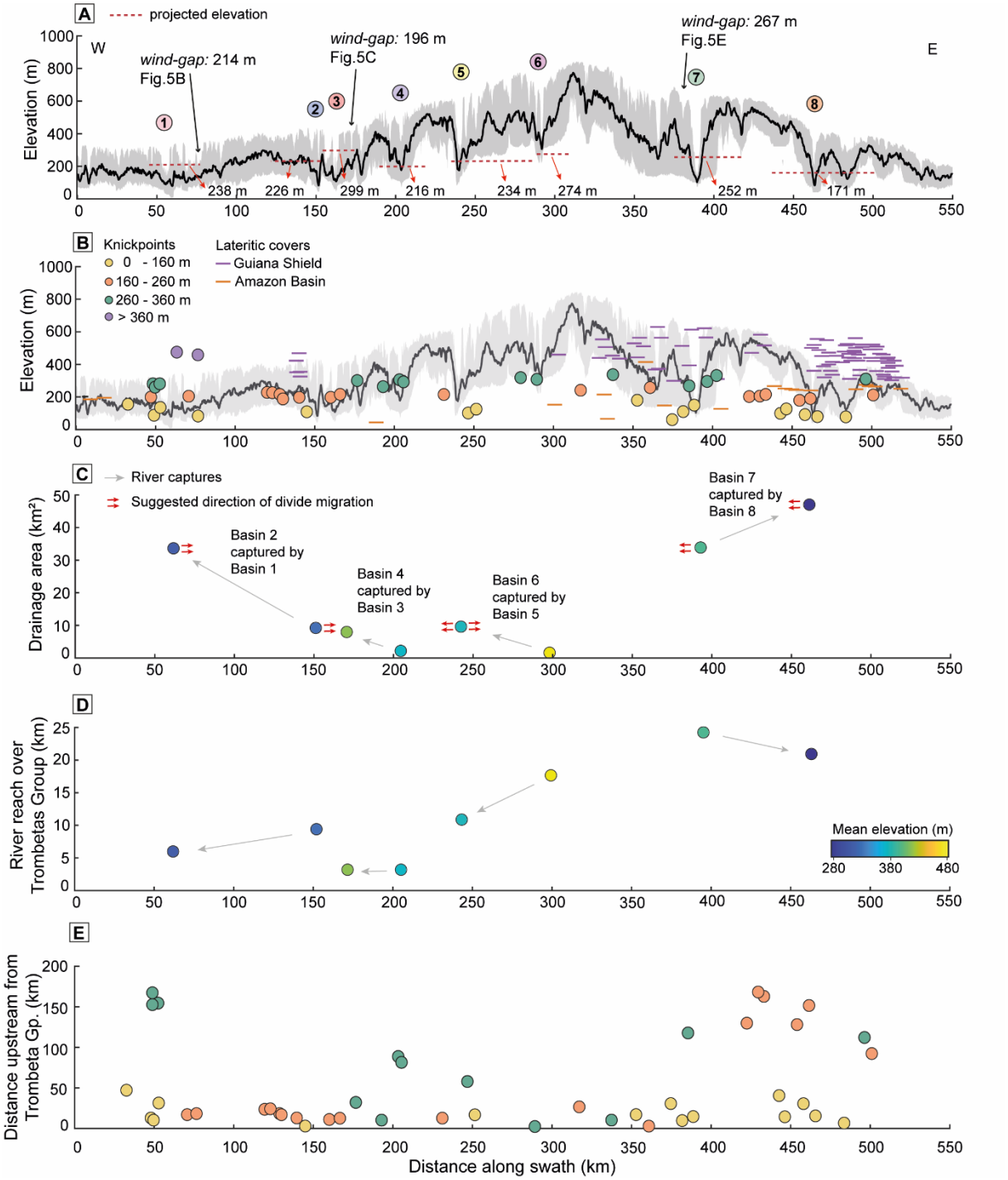

Figure 2.7- Along-strike geomorphic patterns. A) Swath profile of the main escarpment indicating the approximate position of the studied basins. Wind-gap and reconstructed paleo-profile elevations are indicated by black arrows and red dotted lines, respectively (see Fig. 2.5 for map locations). B) Elevation of knickpoints and lateritic surfaces to the north (purple) and south (orange) of the ME. C) Drainage area colored by average elevation (colorbar shown in panel D) of the studied basins. Gray arrows show the direction of drainage area loss and point to the capturing basin. Red arrows suggest the direction of drainage divide migration based on topographic analyses (see Sections 2.4.1 and 2.4.2). D) Along-river distances over the Trombetas Gr. of ME-traversing rivers. Markers are colored by elevation and gray arrows indicate the drainage captures between basins as shown in panel C. E) Knickpoint distances with respect to the ME. Knickpoints more than 200 km north of the ME are not shown.

2.5 DISCUSSION

2.5.1 Ongoing landscape transience in the Guiana Shield

Despite being a cratonic region close to base level (Atlantic Ocean), the study area has geomorphic features indicative of landscape transience. The low-relief and semi-circular regions of basins 7 and 8 upstream of the ME (Figs 2.1A, 2.3A) bounded by high k_{sn} upstream (i.e. near the divide between basins 5 and 7, Fig. 2.4A) and another low k_{sn} and relief upstream, all separated by knickpoints (Fig. 2.3A, 2.4A), suggest these features are erosive pulses associated with base level fall migrating northwards in the Guiana Shield and are consistent with a transient state (e.g. Gallen *et al*., 2011, 2013). The absence of coincidences with lithological variations supports this interpretation (Fig. 2.4B).

We maintain that the geomorphic patterns are consistent with a base level fall common to all studied basins. For example, the relief and k_{sn} near several drainage divides are asymmetric and indicative of basins in the center of the plateau losing area to basins at the outer limits of the plateau which in turn also have asymmetric divides with the neighboring lowland basins (Fig. 2.3, 2.4). The migration of drainage divides suggests the retreat of the plateau-edge escarpments towards the interior of the plateau but also amongst drainages on the plateau as well (Fig. 2.3, 2.4A), generating captures orthogonal to the N-S flow of rivers and associated knickpoints as is the case of basins 1 and 2 (Fig. 2.3B-D; Fig. 2.5). All of these features are consistent with the consumption of elevated regions and plateaus by rivers at lower elevations typical of continental interiors (e.g. Gilbert, 1877; Bishop, 1995; Prince *et al*., 2011; Whipple *et al*., 2017; Giachetta and Willett, 2018; Harel *et al*., 2019; Forte and Whipple, 2019; Schwanghart and Scherler, 2020).

The first three flights of knickpoints (i.e. bounding LSB 1-3) are mainly concentrated in the southern part of the study area (Fig. 2.4) and are sometimes clustered in chi-z space, but a single unifying pattern is difficult to pinpoint (Fig. 2.5). Nonetheless, we posit that these patterns are the consequence of drainage captures occurring within the plateau. For example, capture of upland areas at different locations in the plateau would generate steps on the chi-z plots at variable locations, segmenting the profiles in different LSBs with similar k_{sn} (Fig. 2.5) (see Giachetta and Willett, 2018). Furthermore, except for Basin 6, the trunk streams in all studied basins have steep chi-z profiles at low chi values from which tributaries span out at intermediate elevations with lower k_{sn} (Fig. 2.5). This pattern in which rivers that capture adjacent basins are collapsed into low chi values is consistent with the expected disruption of collinearity between major rivers and their tributaries in chi-z space (Willett *et al*., 2014; Giachetta and Willett, 2018). Basins 2-4 are the best examples of this process, as they belong to the same main channel (e.g. Rio Curuá; see Fig. 2.1A) where Basin 4

(captured by Basin 3) is displaced to higher values of chi while Basin 3 is dislocated to low chi values. Both have knickpoints on the same elevation regardless of the rock type and above which the k_{sn} is similar, suggesting these rivers were once connected (Fig. 2.3E and Fig. 2.5B). Basin 2, in turn captured by Basin 1, is further displaced to high values of chi, also with knickpoints at similar elevations not coinciding with changes in rock type (compare figures 2.4 and 2.5), consistent with the consequences drainage capture (Willett *et al*., 2014; Giachetta and Willett, 2018). Together, the observations point to an ongoing landscape transience in the Guiana Shield.

2.5.2 Geomorphic evidence of lithologic control of base level

Determining a trigger for the widespread divide migration patterns of landscape change in the Guiana shield is challenging. Here, we discuss which mechanisms may have triggered this disequilibrium. Drainage captures result in an increase in the erosion rate at the capture point and generate erosive pulses that propagate towards the headwater, forming radial features in the portion immediately upstream of the capture point as well as excavations in the region downstream (e.g. Gallen *et al*., 2011; Val *et al*., 2014; Gallen, 2018; Giachetta and Willett, 2018). Radial features in the lower portions of basins 7 and 8 and, to a lesser degree, basins 1, 3 and 5 together with the lowering of the average elevation of the ME when cut by these rivers (e.g. Fig. 2.7A) could be interpreted as river captures. In this case, rivers south of the ME would have captured rivers to its north (Hypothesis 1); the ME being a regional drainage divide prior to the modern state (Fig. 2.8A). Despite explaining part of the geomorphic features, this hypothesis is inconsistent with the systematic divide migration patterns and ME-traversing wind-gaps (e.g. Fig. 2.8; Fig. 2.6). Thus, we suggest another plausible mechanism (Hypothesis 2).

The exhumation of resistant lithology in the middle reach of channels increase local slopes (e.g. Forte *et al*., 2016), passively uplifting the areas upstream of the soft-hard rock contact and forming a local base level (e.g. Bernard *et al*., 2021). Differential uplift of a downstream reach generates flattening of river profiles upstream of the uplifted zone due to base level rise (e.g. Adams *et al*., 2016; Ruetenik *et al*., 2016). We observe low relief zones immediately upstream the ME similar to those upstream of uplifting downstream reaches. In the Guiana Shield, these zones might have formed during the exhumation of the resistant lithology in the southern edge of the plateau (Fig. 2.8B).

Hypothesis 2 explains many of the disequilibrium features found on the plateau and suggests a local lithological control of base level of rivers that drain the Guiana Shield. It explains the wind-gaps crossing the ME associated with high k_{sn} (see Fig. 2.4, 2.6). In this scenario, the base level falls nucleated in the Amazon River slowly drove the gradual incision into, and exhumation of the

Trombetas Gr., widening its surface expression (Fig. 2.8B). This interpretation is further supported by the concordance of reconstructed relic reaches and wind-gap elevations on the ME. Interestingly, these elevations are also similar to preserved lateritic surfaces south of the ME (Fig. 2.7A), suggesting a continuous, likely south grading surface through the ME down to the Amazon River.

Hypothesis 2 also explains the divide migration patterns in the Guiana Shield. Knickpoints originating in the Amazon River propagate upstream at speeds directly dependent on the drainage area and with the distance covered over Gr. Trombetas. The larger basins with shorter the distance over the resistant rocks of the Trombetas Gr. (hard rock) would have faster knickpoints according to Equation 4 (e.g. Crosby and Whipple, 2006). We suggest that the Trombetas Gr. acts as knickpoint speedbumps, delaying the propagation of knickpoints travelling upstream from the Amazon River (e.g. Fig. 2.8B) and triggering differential lowering of base levels within neighboring basins in response to the same base level history of the Amazon River. This mechanism explains the along-strike drainage capture, drainage divide migration, and disparity between travelled knickpoint migration distances (Fig. 2.7E).

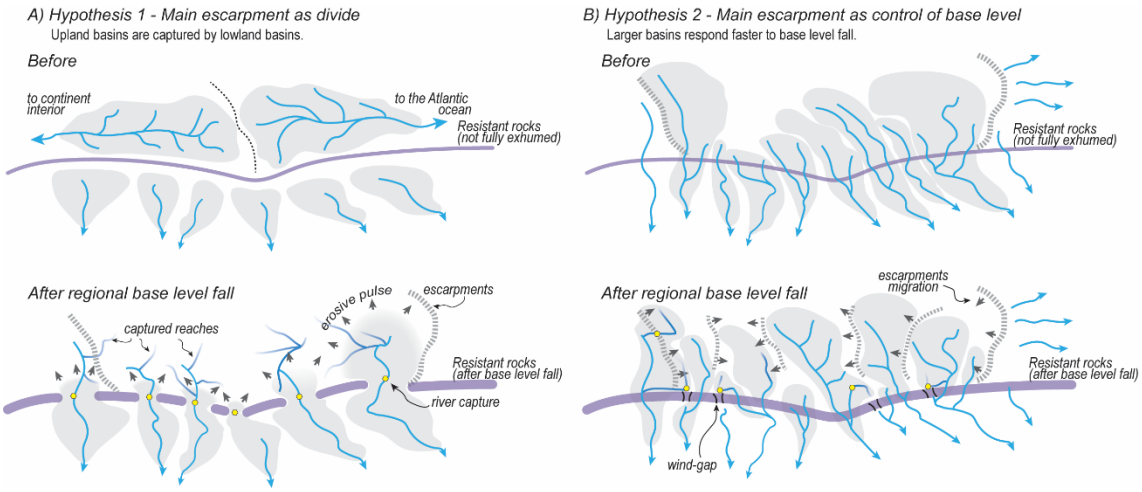

Figure 2.8- Plausible and preferred hypotheses of landscape evolution of the eastern Guiana Shield A) Hypothesis 1: River capture mechanism; plausible. Top: Pre-capture drainage configuration with the ME constituting a drainage divide isolating the Guianas Shield from lowland basins. Below: Post-capture configuration in which sub basins capture the Guianas rivers. B) Hypothesis 2: Lithologic control of base level; preferred. Shield rivers flow in a north-south direction crossing the ME partially exposed on the surface. Slow exhumation of the resistant rocks on the ME act as a local base level control. This process generates profile flattening, erosive pulses, knickpoints, drainage divide migration, and river captures between basins.

2.5.3 Other possible controls of base level

The Trombetas Gr. extends hundreds of kilometers along-strike to the west of the study area and along the northern edge of the Amazon Sedimentary Basin where plateaus similar to the eastern Guiana Shield do not exist. To a lesser extent, the Trombetas Gr. is also exposed along the southern

limit of this basin south of the Amazon River, at the limit with the Brazilian Shield. In both cases, rivers also traverse the same resistant rocks but do not contain an expressive plateau such as the eastern Guiana Shield. Thus, the formation of the plateau itself may need more than resistant lithologies to explain its genesis such as localized surface uplift.

Small amounts of surface uplift may be linked to dynamic topography underneath the plateau, although this observation is model dependent (indirectly shown in Bicudo *et al*., 2020). Furthermore, given the proximity to some of the thickest sections of the Amazon Sedimentary Basin (i.e. Moura et a., 2021), flexural uplift of the ME itself (Nunn *et al*., 1988) may also be another component of uplift driving base level rise in the plateau-exiting streams, contributing to plateau formation. That the reconstruction of Basin 3 points to paleo-outlet elevations higher than the wind-gaps supports plateau uplift (Fig. 2.6C). Importantly, the patterns of drainage reorganization and divide migration amongst neighboring basins occur at much shorter wavelengths compared to a dynamic topography signal. Moreover, the transient patterns are hundreds of kilometers north of the region affected by flexural uplift (Nunn *et al*., 1988). Therefore, while surface uplift may have contributed to the landscape transience, it cannot explain the inner plateau patterns of divide migration and drainage captures.

Flexural uplift of the passive margin in part also caused by the marine sedimentary pile in the Amazon fan also affects the easternmost regions of the Guiana shield (Watts *et al*., 2010). In this case, uplift is highest near the coast and gradually decreases westward. The easternmost basins of the study area (basins 7 and 8) contain the most expressive semi-circular features of excavation in the lower reaches (Fig. 2.4) and may have been influenced by the effects of this flexural uplift. The eastward gain in elevation of lateritic surfaces south of the ME is consistent with this scenario (Fig. 2.7B).

2.5.4 Implications for landscape evolution in the Amazon region and continent interiors

Our results suggest that exhumation of resistant rocks in the Amazon can lead to widespread drainage reorganization and river captures, like post-orogenic landscapes with complex lithology and little tectonic activity (Gallen, 2018, Marques *et al*., 2021). Exhumation of resistant rocks may slowly take place over time as the Amazon River as well as its tributaries slowly excavate their substrate at erosion rates of 5 to 40 m/Ma (Théveniaut and Freyssinet, 1999; Balan *et al*., 2005; Wittmann *et al*, 2011; Allard *et al*., 2018). Superposed changes in base level related to the transcontinentalization in the late Miocene as well as changes sediment flux and Mio-Pliocene and Pleistocene eustatic variations in sea level (see Section 2.2.1) (Figueiredo *et al*., 2009; Irion *et al*.,

2010; Hoorn *et al*., 2010; Gorini *et al*., 2013; Hoorn *et al*., 2017) may have contributed to changes in the base level of the eastern Amazon River, driving incision propagating into the shields via the tributaries. We propose that, as the base level history drives the exhumation of complex lithologic patterns such as in cratonic regions, knickpoint speedbumps may control the rate at which large continental regions respond. This mechanism may play an underconstrained role in the drainage network configuration of the Amazon region as well as other post-orogenic landscapes.

Climatic variations during the Cenozoic favored the formation and development of long-lived lateritic surfaces throughout the Amazon region (Girard *et al*., 2000; Théveniaut and Freyssinet, 2002; Allard *et al*., 2018; Wang *et al*., 2017). Today, these surfaces function as topographic markers and their importance is generally discussed in terms of the stable surfaces that they form. As lateritization processes are typical of tropical regions and form highly resistant horizons near the surface, this pedogenetic process may be an underexplored mechanism not for the preservation of paleosurfaces or pediplains (i.e. Guillocheau *et al*., 2018), but for triggering drainage network reorganizations in tropical continental interiors.

The mechanism of river reorganization described here is not exclusive of tropical regions and may well affect other regions of the world with high contrasts in rock erodibility (e.g. Gallen, 2018; Bernard *et al*., 2021). We maintain that landscapes in continent interiors (i.e. cratons, post-orogenic areas, lowlands) are subject to autogenic river reorganizations as the slow topographic decay (or a post-orogenic uplift mechanism) drives the exhumation of rocks with higher resistance to erosion. The nature of these regions with slow erosion rates might combine to preserve landscape dynamics for millions of years (e.g. Beeson *et al*., 2017; Whipple *et al*., 2017) and constitute natural laboratories for deep time investigation of landscape dynamics.

2.6 CONCLUSIONS

Cratonic regions are the type-examples of stable continental interiors with slow erosion rates. Not surprisingly, these regions are typically thought to be non-changing and unappealing with respect to landscape dynamics. Here, we document widespread geomorphic transients such as drainage captures, drainage divide migration, and wind-gaps in the Guiana Shield of NE Amazonia and demonstrate that these regions might be dynamic after all. We document modification of basin geometry and area in response to lithological complexity. Specifically, resistant lithologies control the position of a main escarpment in the south portion of the Guiana Shield and the response of river basins to base level lowering. We argue that the continued exhumation of a resistant lithology in the lower course of rivers creates a local base level that triggers a transient response of the landscape by slowing down the velocities at which knickpoints (nucleated in a common base level) propagate

upstream. We argue that this process is followed by a series of systematic landscape transients which may be common in cratonic and post-orogenic regions.

The long response times of such regions may keep them from ever reaching topologic equilibrium due to autogenic processes. Though avoided by an expectation of landscape stability, low-relief cratonic landscapes may offer an exceptional natural laboratory to study the landscape response to the exhumation of complex lithological patterns.

This work was funded by Serrapilheira Institute (Grant 1811-25837 to Pedro Val), The Brazilian National Council for Scientific and Technological Development - CNPq (Grant 438735/2018-8 to Pedro Val), and by the Coordination for the Improvement of Higher Education Personnel - CAPES (MSc Scholarship 88882.459377/2019-01 to Camila M. Fadul via Programa de Pós-Graduação em Evolução Crustal e Recursos Naturais (UFOP). We thank Ideflor-Bio and Gil Miranda for logistical support in the field and Pedro Oliveira for assistance in figure production. We thank Daniel Peifer, Fabiano Pupim, and Humberto Reis for discussions that helped improve this manuscript.

All Supporting Information from Chapter 2 (“Ongoing landscape transience in the Eastern Amazon Craton consistent with lithologic control of base level”) is available in the Appendix section.

CÁPITULO 3
CONCLUSÃO

As regiões cratônicas são exemplos de regiões geomorfologicamente estáveis com taxas de erosão lenta. São tipicamente consideradas inalteráveis ao longo do tempo geológico e pouco atraentes no que diz respeito à dinâmica da paisagem. Nesse trabalho, documentamos feições geomórficas indicando transiência da paisagem, como capturas de drenagem, migração de divisão de drenagem, *knickpoints* e *wind-gaps* no Escudo das Guianas, NE da Amazônia, e demonstramos que essas regiões podem ser dinâmicas. Documentamos a modificação da geometria e da área da bacia em resposta à complexidade litológica. Especificamente, as litologias resistentes controlam a posição de uma escarpa principal na porção sul do Escudo das Guianas e a resposta das bacias hidrográficas ao rebaixamento do nível da base. Argumentamos que a exumação contínua de uma litologia resistente no curso inferior dos rios cria um nível de base local que desencadeia uma resposta transitória da paisagem ao diminuir as velocidades nas quais knickpoints (nucleados em um nível de base comum) se propagam à montante. Argumentamos que esse processo é seguido por uma série de transiência sistemática da paisagem que podem ser comuns em regiões cratônicas e pós-orogênicas.

Os longos tempos de resposta dessas regiões podem impedi-las de atingir o equilíbrio topológico devido a processos autogênicos. Embora evitadas por uma expectativa de estabilidade da paisagem, as paisagens cratônicas de baixo relevo podem oferecer um laboratório natural excepcional para estudar a resposta da paisagem à exumação de padrões litológicos complexos.

Referências

Adams, B. A., Whipple, K. X., Hodges , K. V., and Heimsath, A. M., 2016. In situ development of high-elevation, lowrelief landscapes via duplex deformation in the Eastern Himalayan hinterland, Bhutan, J. Geophys. Res. Earth Surf., 121, 294–319, https://doi.org/10.1002/2015JF003508

Allard, T., Gautheron, C., Riffel, S. B., Balan, E., Soares, B. F., Pinna-Jamme, R., Derycke, A., Morin, G., Bueno, G. T., & Do Nascimento, N., 2018. Combined dating of goethites and kaolinites from ferruginous duricrusts. Deciphering the Late Neogene erosion history of Central Amazonia. Chemical Geology, 479, 136-150. https://doi.org/10.1016/j.chemgeo.2018.01.004

Aleva, G. J. J., 1981. Essential differences between the bauxite deposits along the southern and northern edges of the Guiana Shield, South America. Economic Geology, 76(5), 1142-1152. https://doi.org/10.1016/j.chemgeo.2020.119792

Ahnert, F., 1970. Functional relationships between denudation, relief, and uplift in large, mid-latitude drainage basins. American Journal of Science, 268(3), 243-263. https://doi.org/10.2475/ajs.268.3.243

Balan, E., Allard, T., Fritsch, E., Sélo, M., Falguères, C., Chabaux, F., Pierret, M. C., & Calas, G., 2005. Formation and evolution of lateritic profiles in the middle Amazon basin: Insights from radiation-induced defects in kaolinite. Geochimica et Cosmochimica Acta, 69(9), 2193-2204. https://doi.org/10.1016/j.gca.2004.10.028

Beeson, H. W., McCoy, S. W., & Keen-Zebert, A., 2017. Geometric disequilibrium of river basins produces long-lived transient landscapes. Earth and Planetary Science Letters, 475, 34-43. https://doi.org/10.1016/j.epsl.2017.07.010

Berlin, M. M., & Anderson, R. S., 2007. Modeling of knickpoint retreat on the Roan Plateau, western Colorado. Journal of Geophysical Research: Earth Surface, 112(F3). https://doi.org/10.1029/2006jf000553

Bernard, T., Sinclair, H. D., Gailleton, B., & Fox, M., 2021. Formation of Longitudinal River Valleys and the Fixing of Drainage Divides in Response to Exhumation of Crystalline Basement. Geophysical Research Letters, 48(8), e2020GL092210. https://doi.org/10.1029/2020GL092210

Bicudo, T. C., Sacek, V., & de Almeida, R. P., 2020. Reappraisal of the relative importance of dynamic topography and Andean orogeny on Amazon landscape evolution. Earth and Planetary Science Letters, 546, 116423. https://doi.org/10.1016/j.epsl.2020.116423

Bishop, P., 1995. Drainage rearrangement by river capture, beheading and diversion. Progress in

physical geography, 19(4), 449-473. https://doi.org/10.1177/030913339501900402

Boschman, L. M., Cassemiro, F. A., Carraro, L., de Vries, J., Altermatt, F., Hagen, O., Hoorn, C., & Pellissier, L., 2021. South American freshwater fish diversity shaped by Andean uplift since the Late Cretaceous. bioRxiv. https://doi.org/10.1101/2021.05.14.444133

Cordani, U. G., & Teixeira, W., 2007. Proterozoic accretionary belts in the Amazonian Craton. Geological Society of America Memoirs, 200, 297-320. https://doi.org/10.1130/2007.1200(14)

Crosby, B. T., & Whipple, K. X., 2006. Knickpoint initiation and distribution within fluvial networks: 236 waterfalls in the Waipaoa River, North Island, New Zealand. Geomorphology, 82(1-2), 16-38. https://doi.org/10.1016/j.geomorph.2005.08.023

da Costa, M. L., da Silva Cruz, G., de Almeida, H. D. F., & Poellmann, H., 2014. On the geology, mineralogy and geochemistry of the bauxite-bearing regolith in the lower Amazon basin: Evidence of genetic relationships. Journal of Geochemical Exploration, 146, 58-74. https://doi.org/10.1016/j.gexplo.2014.07.021

da Cruz Cunha, P. R., Gonçalves de Melo, J. H., & da Silva, O. B., 2007. Bacia do Amazonas. Boletim de Geociências da PETROBRAS, 15, 227-251.

de Moura Almeida, Y., Marotta, G. S. A., França, G. S., Vidotti, R. M., & Fuck, R. A., 2021. Crustal thickness estimation and tectonic analysis of the Amazonian Craton from gravity data. Journal of South American Earth Sciences, 111, 103449. https://doi.org/10.1016/j.jsames.2021.103449

Dobson, D. M., Dickens, G. R., & Rea, D. K., 2001. Terrigenous sediment on Ceara Rise: a Cenozoic record of South American orogeny and erosion. Palaeogeography, Palaeoclimatology, Palaeoecology, 165(3-4), 215-229. https://doi.org/10.1016/s0031-0182(00)00161-9

dos Santos Albuquerque, M. F., Horbe, A. M. C., & Danišík, M., 2020. Episodic weathering in Southwestern Amazonia based on (UTh)/He dating of Fe and Mn lateritic duricrust. Chemical Geology, 553, 119792. https://doi.org/10.1016/j.chemgeo.2020.119792

Farr, T.G., Rosen, P.A., Caro, E., Crippen, R., Duren, R., Hensley, S., Kobrick, M., Paller, M., Rodriguez, E., Roth, L., Seal, D., Shaffer, S., Shimada, J., Umland, J., Werner, M., Oskin, M., Burbank, D., Alsdorf, D., 2007. The Shuttle Radar Topography Mission, Rev. Geophys., 45, RG2004. https://doi.org/10.1029/2005RG000183

Ferron, J. M. T., Neto, A. C. B., Lima, E. F., Nardi, L. V., Costi, H. T., Pierosan, R., & Prado, M., 2010. Petrology, geochemistry, and geochronology of Paleoproterozoic volcanic and granitic rocks (1.89–1.88 Ga) of the Pitinga Province, Amazonian Craton, Brazil. Journal of south American earth sciences, 29(2), 483-497.

Figueiredo, J. J. J. P., Hoorn, C., Van der Ven, P., & Soares, E., 2009. Late Miocene onset of the Amazon River and the Amazon deep-sea fan: Evidence from the Foz do Amazonas Basin. Geology, 37(7), 619-622. https://doi.org/10.1130/G25567A

Flint, J. J., 1974. Stream gradient as a function of order, magnitude, and discharge. Water Resources Research, 10(5), 969-973. https://doi.org/10.1029/WR010i005p00969

Forte, A. M., Yanites, B. J., & Whipple, K. X., 2016. Complexities of landscape evolution during incision through layered stratigraphy with contrasts in rock strength. Earth Surface Processes and Landforms, 41(12), 1736-1757. https://doi.org/10.1002/esp.3947

Forte, A. M., & Whipple, K. X., 2018. Criteria and tools for determining drainage divide stability. Earth and Planetary Science Letters, 493, 102-117. https://doi.org/10.1016/j.epsl.2018.04.026

Forte, A. M., & Whipple, K. X., 2019. The Topographic Analysis Kit (TAK) for TopoToolbox. Earth Surface Dynamics, 7(1), 87-95. https://doi.org/10.5194/esurf-7-87-2019, 2019.

Gallen, S. F., Wegmann, K. W., Frankel, K. L., Hughes, S., Lewis, R. Q., Lyons, N., ... & Witt, A. C., 2011. Hillslope response to knickpoint migration in the Southern Appalachians: implications for the evolution of post-orogenic landscapes. Earth Surface Processes and Landforms, 36(9), 1254-1267. https://doi.org/10.1002/esp.2150

Gallen, S. F., Wegmann, K. W., & Bohnenstiehl, D. R., 2013. Miocene rejuvenation of topographic relief in the southern Appalachians. GSA Today, 23(2), 4-10. https://doi.org/10.1130/GSATG163A.1

Gallen, S. F., 2018. Lithologic controls on landscape dynamics and aquatic species evolution in post-orogenic mountains. Earth and Planetary Science Letters, 493, 150-160. https://doi.org/10.1016/j.epsl.2018.04.029.

Giachetta, E., & Willett, S. D., 2018. Effects of river capture and sediment flux on the evolution of plateaus: Insights from numerical modeling and river profile analysis in the upper Blue Nile catchment. Journal of Geophysical Research: Earth Surface, 123, 1187–1217. https://doi.org/10.1029/2017JF004252

Gilbert, G. K., 1877. Geology of the Henry mountains (pp. i-160). Government Printing Office.

Girard, J. P., Razanadranorosoa, D., & Freyssinet, P., 1997. Laser oxygen isotope analysis of weathering goethite from the lateritic profile of Yaou, French Guiana: paleoweathering and paleoclimatic implications. Applied Geochemistry, 12(2), 163-174. https://doi.org/10.1016/S0016-7037(99)00299-9

Gorini, C., Haq, B. U., dos Reis, A. T., Silva, C. G., Cruz, A., Soares, E., & Grangeon, D., 2014. Late Neogene sequence stratigraphic evolution of the Foz do Amazonas Basin, Brazil. Terra Nova, 26(3), 179-185. https://doi.org/10.1111/ter.12083

Grubb, P. L. C., 1979. Genesis of bauxite deposits in the lower Amazon basin and Guianas coastal plain. Economic Geology, 74(4), 735-750. https://doi.org/10.2113/gsecongeo.74.4.735

Guillocheau, F., Simon, B., Baby, G., Bessin, P., Robin, C., & Dauteuil, O., 2018. Planation surfaces as a record of mantle dynamics: the case example of Africa. Gondwana Research, 53, 82-98. https://doi.org/10.1016/j.gr.2017.05.015

Harbor, D., Bacastow, A., Heath, A. W., & Rogers, J., 2005. Capturing variable knickpoint retreat in the Central Appalachians, USA. Geografia Fisica e Dinamica Quaternaria, 28(1), 23-36.

Harel, E., Goren, L., Shelef, E., & Ginat, H., 2019. Drainage reversal toward cliffs induced by lateral lithologic differences. Geology, 47(10), 928-932. https://doi.org/10.1130/G46353.1

Hoorn, C., Wesselingh, F. P., Ter Steege, H., Bermudez, M. A., Mora, A., Sevink, J., Sanmartín, I., Sanchez-Meseguer, A., Anderson, C. L., Figueiredo, J. P., Jaramillo, C., Riff, D., Negri, F. R., Hooghiemstra, H., Lundberg, J., Stadler, T., Särkinen, T., & Antonelli, A., 2010. Amazonia through time: Andean uplift, climate change, landscape evolution, and biodiversity. science, 330(6006), 927-931. https://doi.org/10.1126 /science.1194585

Hoorn, C., Bogotá-A, G. R., Romero-Baez, M., Lammertsma, E. I., Flantua, S. G., Dantas, E. L., & Chemale Jr, F., 2017. The Amazon at sea: Onset and stages of the Amazon River from a marine record, with special reference to Neogene plant turnover in the drainage basin. Global and Planetary Change, 153, 51-65. https://doi.org/10.1016/j.gloplacha.2017.02.005

Irion, G., Müller, J., Morais, J. O., Keim, G., de Mello, J. N., & Junk, W. J., 2009. The impact of Quaternary sea level changes on the evolution of the Amazonian lowland. Hydrological Processes: An International Journal, 23(22), 3168-3172. https://doi.org/10.1002/hyp.7386

Japan Aerospace Exploration Agency, 2021. ALOS World 3D 30 meter DEM. V3.2, Jan 2021. Distributed by OpenTopography. https://doi.org/10.5069/G94M92HB Accessed: 2021-11-08

Lague, D., 2014. The stream power river incision model: evidence, theory and beyond. Earth Surface Processes and Landforms, 39(1), 38-61. https://doi.org/10.1002/esp.3462.

Marques, K. P. P., dos Santos, M., Peifer, D., da Silva, C. L., & Vidal-Torrado, P., 2021. Transient and relict landforms in a lithologically heterogeneous post-orogenic landscape in the intertropical belt (Alto Paranaíba region, Brazil). Geomorphology, 391, 107892. https://doi.org/10.1016/j.geomorph.2021.10789

Nunn, J. A., & Aires, J. R., 1988. Gravity anomalies and flexure of the lithosphere at the Middle Amazon Basin, Brazil. Journal of Geophysical Research: Solid Earth, 93(B1), 415-428. https://doi.org/10.1029/jb093ib01p00415

Peixoto, S. F., & Horbe, A. M. C., 2008. Bauxitas do nordeste do Amazonas. Brazilian Journal of Geology, 38(2), 406-422.

Perne, M., Covington, M. D., Thaler, E. A., & Myre, J. M., 2017. Steady state, erosional continuity, and the topography of landscapes developed in layered rocks. Earth Surface Dynamics, 5(1), 85-100. https://doi.org/10.5194/esurf-5-85-2017.

Perron, J. T., & Royden, L., 2013. An integral approach to bedrock river profile analysis. Earth Surface Processes and Landforms, 38(6), 570-576. https://doi.org/10.1002/esp.3302

Pupim, F. N., Sawakuchi, A. O., Almeida, R. P. D., Ribas, C. C., Kern, A. K., Hartmann, G. A., Chiessie, C. M., Tamura, L. N., Mineli, T. D., Savian, J.F., Grohmann, D. J., Bertassoli, Jr., Stern, A. G., Cruz, F. W., & Cracraft, J., 2019. Chronology of Terra Firme formation in Amazonian lowlands reveals a dynamic Quaternary landscape. Quaternary Science Reviews, 210, 154-163. https://doi.org/10.1016/j.quascirev.2019.03.008

Prince, P. S., Spotila, J. A., & Henika, W. S., 2011. Stream capture as driver of transient landscape evolution in a tectonically quiescent setting. Geology, 39(9), 823-826. https://doi.org/10.1130/G32008.1

Rosenbloom, N. A., & Anderson, R. S., 1994. Hillslope and channel evolution in a marine terraced landscape, Santa Cruz, California. Journal of Geophysical Research: Solid Earth, 99(B7), 14013-14029. https://doi.org/10.1029/94JB00048

Rossetti, D. F., Cohen, M. C., Tatumi, S. H., Sawakuchi, A. O., Cremon, É. H., Mittani, J. C., Bertani, T. C., Munita, C. J. A. S., Tudela, D. R. G, Yee, M., & Moya, G., 2015. Mid-Late Pleistocene OSL chronology in western Amazonia and implications for the transcontinental Amazon pathway. Sedimentary Geology, 330, 1-15. https://doi.org/10.1016/j.sedgeo.2015.10.001

Ruetenik, G. A., Hoke, G. D., Moucha, R., & Val, P., 2018. Regional landscape response to thrust belt dynamics: The Iglesia basin, Argentina. Basin Research, 30(6), 1141-1154. https://doi.org/10.1111/bre.12295

Sacek, V., 2014. Drainage reversal of the Amazon River due to the coupling of surface and lithospheric processes. Earth and Planetary Science Letters, 401, 301-312. ttps://doi.org/10.1016/j.epsl.2014.06.022

Scotese, C. R., 2009. Late Proterozoic plate tectonics and palaeogeography: a tale of two

supercontinents, Rodinia and Pannotia. Geological Society, London, Special Publications, 326(1), 67-83.

Shephard, G. E., Müller, R. D., Liu, L., & Gurnis, M., 2010. Miocene drainage reversal of the Amazon River driven by plate–mantle interaction. Nature Geoscience, 3(12), 870-875. https://doi.org/10.1038/NGEO101

Schwanghart, W., & Scherler, D., 2014. TopoToolbox 2–MATLAB-based software for topographic analysis and modeling in Earth surface sciences. Earth Surface Dynamics, 2(1), 1-7. https://doi.org/10.5194/esurf-2-1-2014

Schwanghart, W., & Scherler, D., 2017. Bumps in river profiles: uncertainty assessment and smoothing using quantile regression techniques. Earth Surface Dynamics, 5(4), 821-839. https://doi.org/10.5194/esurf-5-821-2017, 2017

Schwanghart, W., & Scherler, D., 2020. Divide mobility controls knickpoint migration on the Roan Plateau (Colorado, USA). Geology, 48(7), 698-702. https://doi.org/10.1130/G47054.1

Théveniaut, H., & Freyssinet, P., 1999. Paleomagnetism applied to lateritic profiles to assess saprolite and duricrust formation processes: the example of Mont Baduel profile (French Guiana). Palaeogeography, Palaeoclimatology, Palaeoecology, 148(4), 209-231. https://doi.org/10.1016/s0031-0182(98)00183-7

Théveniaut, H., & Freyssinet, P. H., 2002. Timing of lateritization on the Guiana Shield: synthesis of paleomagnetic results from French Guiana and Suriname. Palaeogeography, Palaeoclimatology, Palaeoecology, 178(1-2), 91-117. https://doi.org/10.1016/S0031-0182(01)00404-7

Val, P., Silva, C., Harbor, D., Morales, N., Amaral, F., & Maia, T., 2014. Erosion of an active fault scarp leads to drainage capture in the Amazon region, Brazil. Earth Surface Processes and Landforms, 39(8), 1062-1074. https://doi.org/10.1002/esp.3507

van Soelen, E. E., Kim, J. H., Santos, R. V., Dantas, E. L., de Almeida, F. V., Pires, J. P., ... & Damsté, J. S. S., 2017. A 30 Ma history of the Amazon River inferred from terrigenous sediments and organic matter on the Ceará Rise. Earth and Planetary Science Letters, 474, 40-48. https://doi.org/10.1016/j.epsl.2017.06.025

Wanderley-Filho, J. R., Eiras, J. F., da Cruz Cunha, P. R., & van der Ven, P. H., 2010. The Paleozoic Solimões and Amazonas basins and the Acre foreland basin of Brazil. Amazonia: Landscape and Species Evolution: A look into the past, 29-37. https://doi.org/10.1002/9781444306408.ch3

Wang, X., Edwards, R. L., Auler, A. S., Cheng, H., Kong, X., Wang, Y., Cruz, F. W., Dorale, J. A., & Chiang, H. W., 2017. Hydroclimate changes across the Amazon lowlands over the past 45,000

years. Nature, 541(7636), 204-207. https://doi.org/10.1038/nature20787

Watts, A. B., Rodger, M., Peirce, C., Greenroyd, C. J., & Hobbs, R. W., 2009. Seismic structure, gravity anomalies, and flexure of the Amazon continental margin, NE Brazil. Journal of Geophysical Research: Solid Earth, 114(B7). https://doi.org/10.1029/2008JB006259

Whipple, K. X., & Tucker, G. E., 1999. Dynamics of the stream-power river incision model: Implications for height limits of mountain ranges, landscape response timescales, and research needs. Journal of Geophysical Research: Solid Earth, 104(B8), 17661-17674. https://doi.org/10.1029 /1999JB900120

Whipple, K. X., 2001. Fluvial landscape response time: How plausible is steady-state denudation?. American Journal of Science, 301(4-5), 313-325. https://doi.org/10.2475/ajs.301.4-5.313

Whipple, K. X., Dibiase, R. A., & Crosby, B. T., 2013. Bedrock rivers. In Fluvial Geomorphology (pp. 550-573). Elsevier Inc. https://doi.org/10.1016/B978-0-12-374739-6.00254-2

Whipple, K. X., DiBiase, R. A., Ouimet, W. B., & Forte, A. M., 2017. Preservation or piracy: Diagnosing low-relief, high-elevation surface formation mechanisms. Geology, 45(1), 91-94. https://doi.org/10.1130/G38490.1

Willett, S. D., McCoy, S. W., Perron, J. T., Goren, L., & Chen, C. Y., 2014. Dynamic reorganization of river basins. Science, 343(6175). https://doi.org/10.1126/science.1248765

Wittmann, H., von Blanckenburg, F., Maurice, L., Guyot, J. L., Filizola, N., & Kubik, P. W., 2011. Sediment production and delivery in the Amazon River basin quantified by in situ–produced cosmogenic nuclides and recent river loads. Bulletin, 123(5-6), 934-950. https://doi.org/10.1130/B30317.1

Wolpert, J. A., & Forte, A. M., 2021. Response of transient rock uplift and base level knickpoints to erosional efficiency contrasts in bedrock streams. Earth Surface Processes and Landforms, 46(10), 2092-2109. https://doi.org/10.1016/j.epsl.2018.04.026

Apêndice

Supporting Information for

Ongoing landscape transience in the Eastern Amazon Craton consistent with lithologic control of base level

Contents of this file

Table S1

Figure S1

Introduction

This supporting information provides chi-plots for different values of θ (Fig. S1) and constraints on θ (Table S1) using Topotoolbox's mnoptimvar function (Schwanghart and Scherler, 2014).

Table S1. Theta estimates using the mnoptimvar function

Basins	mnoptimvar
1	0.2594
2	0.4906
3	0.4392
4	0.4044
5	0.2823
6	0.3055
7	0.1011
8	0.3702
Avarage ± Mean deviation	0.3316 ± 0.1225

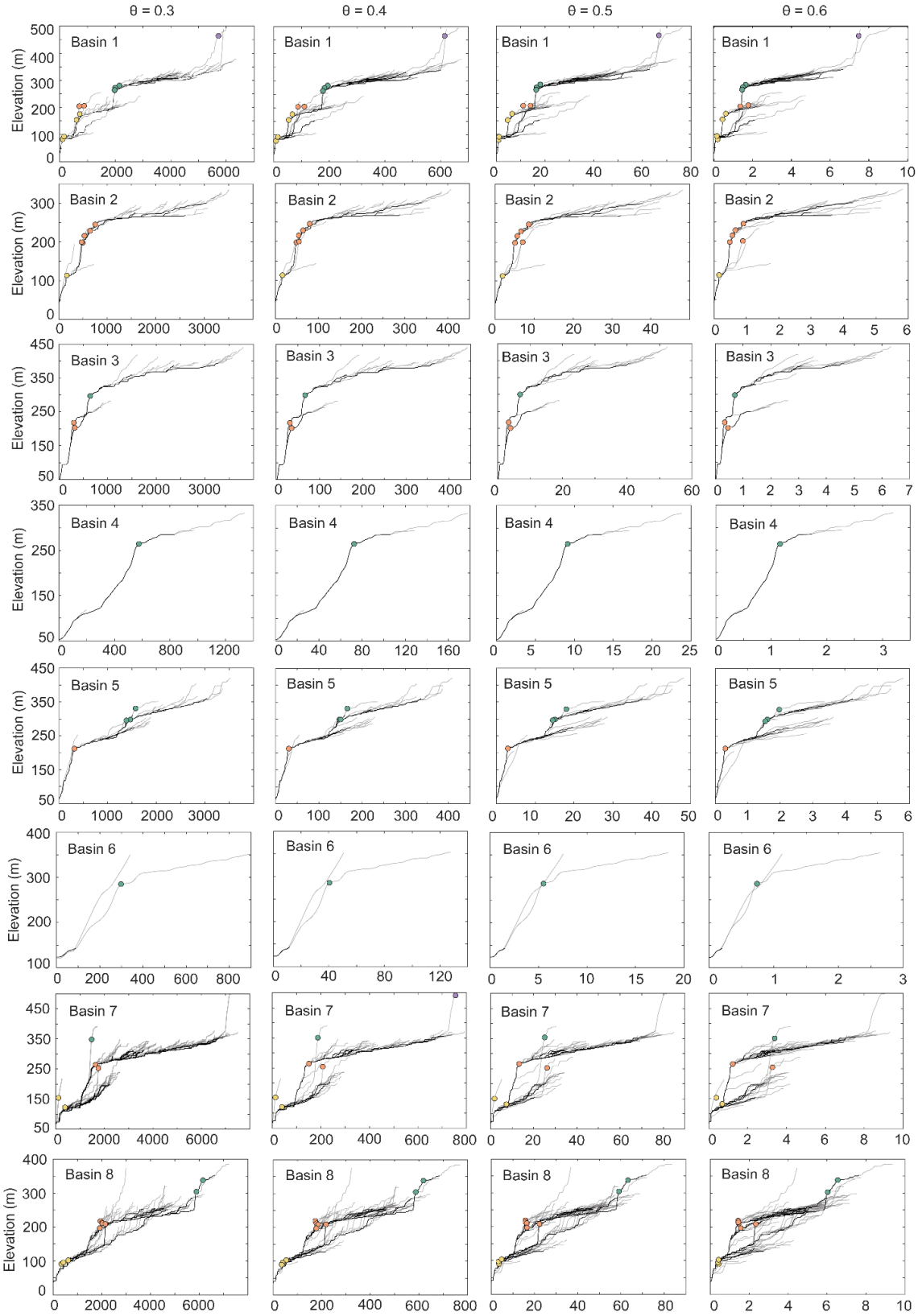

Figure S1. Chi-plot with θ = 0.3, θ = 0.4, θ = 0.5 and θ = 0.6 applied to all basins (1 - 8) analyzed in the Guiana Shield.

References cited

Schwanghart, W., & Scherler, D. (2017). Bumps in river profiles: uncertainty assessment and smoothing using quantile regression techniques. Earth Surface Dynamics, 5(4), 821-839. https://doi.org/10.5194/esurf-5-821-2017, 2017